Available online at www.sciencedirect.com

SCIENCE DIRECT

Developmental Biology 274 (2004) 348–369

DEVELOPMENTAL BIOLOGY

www.elsevier.com/locate/ydbio

The epaxial–hypaxial subdivision of the avian somite

Louise Cheng[1], Lúcia E. Alvares, Mohi U. Ahmed, Amira S. El-Hanfy, Susanne Dietrich*

Department of Craniofacial Development, King's College London, London Bridge, London SE1 9RT, UK

Received for publication 10 February 2003, revised 6 July 2004, accepted 7 July 2004
Available online 23 August 2004

Abstract

In all jaw-bearing vertebrates, three-dimensional mobility relies on segregated, separately innervated epaxial and hypaxial skeletal muscles. In amniotes, these muscles form from the morphologically continuous dermomyotome and myotome, whose epaxial–hypaxial subdivision and hence the formation of distinct epaxial–hypaxial muscles is not understood.

Here we show that *En1* expression labels a central subdomain of the avian dermomyotome, medially abutting the expression domain of the lead-lateral or hypaxial marker *Sim1*. *En1* expression is maintained when cells from the *En1*-positive dermomyotome enter the myotome and dermatome, thereby superimposing the *En1–Sim1* expression boundary onto the developing musculature and dermis.

En1 cells originate from the dorsomedial edge of the somite. Their development is under positive control by notochord and floor plate (Shh), dorsal neural tube (Wnt1) and surface ectoderm (Wnt1-like signalling activity) but negatively regulated by the lateral plate mesoderm (BMP4). This dependence on epaxial signals and suppression by hypaxial signals places *En1* into the epaxial somitic programme. Consequently, the *En1–Sim1* expression boundary marks the epaxial–hypaxial dermomyotomal or myotomal boundary.

In cell aggregation assays, *En1*- and *Sim1*-expressing cells sort out, suggesting that the *En1–Sim1* expression boundary may represent a true compartment boundary, foreshadowing the epaxial–hypaxial segregation of muscle.

Keywords: Chick embryo; Somite; Dermomyotome; Myotome; Dermatome; Skeletal muscle; Epaxial; Hypaxial; Horizontal myoseptum; Cell sorting; *En1*; *Sim1*; *Alx4*; *Shh*; *Wnt*; *BMP4*

Introduction

In higher (gnathostome) vertebrates, locomotion is brought about by a complex array of skeletal muscles (reviewed by Goodrich, 1958). Based on their innervation pattern, we distinguish the dorsally located epaxials, innervated by the dorsal ramus of the spinal nerves and the superficially, laterally and ventrally located hypaxials, innervated by the ventral ramus of the spinal nerves. In amniotes, epaxial muscles are the deep muscles of the back, while the hypaxial muscles include the muscles of the body wall and limbs. For the hypaxials, a further subdivision has been suggested as some complete their development deep within the lateral mesoderm while others remain outside (Burke and Nowicki, 2003). However, all hypaxial muscles are united in that they are physically segregated from the epaxial musculature by a connective tissue sheet termed horizontal myoseptum in fishes, septum laterale in amniotes and fascia thoracolumbalis or lumbodorsal fascia in humans (Goodrich, 1958; Gray, 1995).

In the trunk, all skeletal muscles stem from the segmented paraxial mesoderm, the somites, which in gnathostomes form via the same segmentation mechanism (reviewed by Christ and Ordahl, 1995; Gossler and Hrabe de Angelis, 1998; Pourquié, 2003). It is therefore the more astonishing that muscle formation and, in particular, the epaxial–hypaxial segregation of muscle differ considerably. In the zebrafish embryo for example, most of the somite readily differentiates into embryonic muscle termed myo-

* Corresponding author. Department of Craniofacial Development, King's College London, Floor 27 Guy's Tower, Guy's Hospital, London Bridge, London SE1 9RT, UK. Fax: +44 171 955 2704.
E-mail address: susanne.dietrich@kcl.ac.uk (S. Dietrich).
[1] Present address: MRC National Institute for Medial Research, The Ridgeway, Mill Hill, London NW7 1AA, UK.

0012-1606/$ - see front matter © 2004 Elsevier Inc. All rights reserved.
doi:10.1016/j.ydbio.2004.07.020

tome, which in turn gives rise to the fast-twitch muscles of the juvenile and adult (reviewed by Stickney et al., 2000). A specialised cell population, which initially is located close to axial midline tissues notochord and neural tube and hence is referred to as adaxial cells, migrates through the myotome to form the superficial layer of slow-twitch muscles. However, a subpopulation of these adaxial cells, often termed "muscle pioneers" and distinguished by their expression of the *Engrailed* genes and their dependence on persistent and high-level Shh signalling from the notochord, remains stretched out in a horizontal plane between the notochord and the surface ectoderm (Currie and Ingham, 1996; Ekker et al., 1992; Felsenfeld et al., 1991; Halpern et al., 1993; Hatta et al., 1991; Wolff et al., 2003). These cells form the first, morphologically and molecularly defined epaxial–hypaxial boundary, subsequently organising the formation of the horizontal myoseptum.

In amniotes such as mouse and chick embryos, the somites first differentiate into dermomyotome, the source of muscle and dorsal dermis and sclerotome, the source of vertebral column and ribs (reviewed by Christ and Ordahl, 1995; Gossler and Hrabe de Angelis, 1998). The dermomyotome releases myoblasts from its edges or lips in waves; these cells assemble underneath to form the myotome, while the dermomyotome proper deepithelialises to form the anlage of the dorsal dermis, the dermatome (Christ et al., 1983; Cinnamon et al., 1999, 2001; Denetclaw and Ordahl, 2000; Denetclaw et al., 1997, 2001; Huang and Christ, 2000; Kahane et al., 1998a,b, 2002; Ordahl et al., 2001). Importantly, dermomyotome, myotome and dermatome are continuous structures, and no morphologically defined subdivision into epaxial and hypaxial domains is visible. The epaxial and hypaxial muscle precursors, however, seem to represent distinct lineages (Eloy-Trinquet and Nicolas, 2002; Freitas et al., 2001; Ordahl and Le Douarin, 1992; Selleck and Stern, 1991), with the epaxials arising from the dorsomedial somite quadrant under the control of notochord and dorsal neural tube (reviewed by Brent and Tabin, 2002) and the hypaxials arising from the dorsolateral somite quadrant under the control of surface ectoderm and lateral plate mesoderm (reviewed by Parkyn et al., 2002). Thus, the sites of epaxial–hypaxial myogenesis are distinct, and it has been speculated that this rendered the formation of a specialised epaxial–hypaxial boundary dispensable.

It has to be taken into account, however, that in order to ultimately generate segregated and separately innervated epaxial and hypaxial muscles, also the amniote must have means to define the epaxial–hypaxial border and to prevent the intermingling of the epaxial and hypaxial precursor cells. Thus, an epaxial–hypaxial boundary must exist, even though it is morphologically ill defined. In support of this view, a horizontal subdivision of the dermomyotome and myotome into a dorsal, central or "intercalated" and ventral territory has been proposed, based on the distinct *cis*-regulatory elements controlling the expression of the muscle determining factor Myf5 (Hadchouel et al., 2003) and the expression patterns of the transcription factors En1, Sim1 and Alx4 (Davis et al., 1991; Gardner and Barald, 1992; Ikeya and Takada, 1998; Logan et al., 1992; Olivera-Martinez et al., 2002; Pourquié et al., 1996; Spörle, 2001; Takahashi et al., 1998; Wurst et al., 1994). However, some studies see En1, Sim1 and Alx4 as central markers (Ikeya and Takada, 1998; Spörle, 2001; Takahashi et al., 1998), while others identified Sim1 as lateral and hence hypaxial marker (Pourquié et al., 1996). Thus, neither the association of molecular markers with epaxial–hypaxial somitic programmes nor the mechanisms underlying the segregation of epaxial–hypaxial cells are understood.

In this study, we combined a comparative expression analysis with lineage tracing by DiI–DiO labelling and quail-chick grafting. We show that *Alx4* demarcates the central dermomyotome and later, the dermatome. *En1* and *Sim1* in turn mark subdomains of the *Alx4* territory, with *En1* labelling the epaxial and *Sim1* the hypaxial portion. Importantly, *En1* and *Sim1* expressions continue in myotome and dermatome, such that the molecular boundary is superimposed onto muscle and dermis. Using in ovo microsurgery, we demonstrate that *En1* expression is controlled by a complex regulatory network, with notochord (Shh) and dorsal neural tube (Wnt1) specifying the cells as part of the epaxial precursor pool, the surface ectoderm via Wnt1-like signalling initiating and maintaining *En1* expression and finally, the lateral mesoderm (BMP4) suppressing *En1* expression. Using cell aggregation assays, we show that *En1*- and *Sim1*-expressing dermomyotome cells sort, suggesting that in the embryo, they form a functional epaxial–hypaxial compartment boundary.

Materials and methods

Chick embryos and somite nomenclature

Fertilised chicken and quail eggs (Winter Farm, Royston, Potter Farm, Woodhurst) were incubated at 38.5°C in a humidified incubator and staged according to Hamburger and Hamilton (1951). The developmental age of somites was determined, using the staging system by Christ and Ordahl (1995), modified by Pourquié (1999).

Microsurgery

In ovo ablation of tissues surrounding the paraxial mesoderm and rotation of neural tube and floor plate were performed as described in Dietrich et al. (1997, 1998), using flame-sharpened tungsten needles and Dispase treatment. To graft longitudinal fragments of segmental plates, surface ectoderm plus segmental plate of host (in ovo) and donor [pinned down in a Sylgard (Dow Corning) dish] were cut at the desired position within the segmental plate and at the border of it with tungsten needles, followed by the application of 1–2 μl of 1 mg/ml Dispase (Sigma) to the

cuts. When the desired part of the segmental plate became loose in the host, it was manoeuvred out of the embryo and discarded. The segmental plate portion to be grafted from the host was aspirated into a glass capillary, then release into the slit within the host and manoeuvred into place with tungsten needles. Affigel beads (Biorad) were soaked in 500 μg/ml recombinant Shh protein or 10 or 100 μg/ml recombinant BMP4 protein (R&D) or in 1 mg/ml BSA over night at 4°C, washed in PBS and implanted as indicated schematically in Figs. 4 and 7. To graft control cells or cell-expressing Wnt factors, the cells were trypsinised, incubated in DMEM (Sigma)/20 μM Celltracker Orange (Molecular Probes) on a bacterial plate for 30 min at 37°C, washed twice in DMEM and incubated on a bacterial dish in DMEM over night to allow the formation of cell aggregates (37°C RatB1a cells, 39°C DF1 cells). The aggregates were collected with a micropipette, spun at 800 rpm for 5 min, resuspended in PBS in ice, cut to size and transferred into the host embryos, using serum-coated pipette tips.

Tissue culture

RatB1a control cells carrying the empty expression vector and RatB1a cells expressing mouse Wnt1/5a/5b/6/7a (kindly provided and expression-tested by Western blotting by A. Münsterberg) were cultivated in the presence of G418 (Invitrogen) as described by Fan et al. (1997) and Münsterberg et al. (1995). Furthermore, DF1 cells (ATCC catalogue No. CRL-12203) were transiently transfected with two types of *Wnt6* expression constructs via calcium precipitation: (a) a retroviral RCAS-BP(A) construct harbouring the open reading frame of mouse *Wnt6*, and (b) a pCAβ expression construct of the type described in Alvares et al. (2003), harbouring the ORF of mouse *Wnt6* plus N-terminal Myc-tag, an internal ribosomal entry site and the coding sequence of eGFP. Expression levels of the transfected cells were controlled by RT-PCR using mouse Wnt6-specific primers, by analysing for eGFP-mediated fluorescence (pCAβ-construct) and by immunohistochemistry using an anti-Myc antibody (Invitrogen). In the embryo, the *Wnt6*-expressing RatB1a cells and DF1 cells gave identical results.

DiI/DiO labelling

Two methods were used to apply the fluorescent vital dyes DiI and DiO (Molecular Probes). (a) The dyes were diluted in dimethylformamide (Fluka) to 0.2% and iontophoretically applied to somites I–II, V and X of HH14 embryos as described by Denetclaw et al. (1997). (b) Stock solutions of 0.5% DiI and 0.25% DiO in ethanol were 1:10 diluted in vegetable oil, droplets of 1–2 μm diameter were injected to the somites (same sites as in a, and then aspirated; Ruiz I Altaba et al., 1993). Both types of labelling were performed under an Olympus SZX12 fluorescent stereomicroscope and led to the same results.

Cell aggregation

The cell aggregation procedure followed essentially Wizenmann and Lumsden (1997). Briefly, 200 HH20 dermomyotomes stages X–XX (i.e., of 10 embryos) were excised with tungsten needles, cleaned from adhering tissues using 100 μg/ml Dispase in PBS (Sigma) and horizontally cut, using the known expression boundaries of *En1/Sim1* in HH20 embryos as a guide. To control the appropriateness of the cuts, 8–10 epaxial and hypaxial dermomyotome fragments were embedded in collagen and hybridised with probes for *En1* or *Sim1*. Two thirds of the remaining epaxial and all of the hypaxial fragments (compensating for the smaller size of the hypaxial fragments) were collected in L15 medium (Invitrogen) in separate Petri dishes on ice, washed with F12 medium (Invitrogen) and transferred to a 96-well plate in 200 μl F12. Here, the fragments were incubated for 30 min at 37°C in F12 containing either 20 μM Celltracker Orange or Celltracker Green (Molecular Probes). The preparations were then washed twice in F12, once in calcium-free HBBS (Invitrogen), and combined in a clear PCR tube. To obtain single cell suspensions, two methods were used. Either, the dermomyotome fragments were incubated in 0.02% EDTA in calcium-free HBBS for 5 min and pipetted up and down with serum-coated tips. Alternatively, the fragments were dissociated using a tissue culture mortar and pestle with a clearance of 100 μm. After either type of cell dissociation, the suspensions were passed though a 40-μm filter (BD Falcon) to remove remaining cell clumps. An aliquot of the cell suspension was examined under a Zeiss Axioskop for the incorporation of fluorescent label and the completeness of cell dissociation. The remaining cells were pelleted for 5 min at 200 rpm and resuspended in 200 μl DMEM supplemented with 10% FBS, 2% chick serum and 1% Pen/Strep (Gibco). Ten microliters of this suspension was removed and diluted 1:1000 to determine the cell concentration. The cells were then pelleted and resuspended in DMEM, 10% FBS, 2% chick serum and 1% Pen/Strep to a concentration of 2×10^4 cells/ml. Two hundred microliters of this suspension was transferred into a cloning ring (0.9 cm diameter) glued onto a petridish and cultured on a shaking platform at 65 rpm in a CO_2 incubator at 37°C for 4 h. Once the aggregates had formed, 20 μl of 40% formaldehyde was added for fixation. The aggregates were transferred onto a dipped slide and examined under both a Zeiss Axioskop and a Leica SP1 confocal microscope.

Quantification of cell–cell contacts in cell aggregates

To quantify the extent of cell sorting or mixing, aggregates of the epaxial–hypaxial, epaxial–epaxial and hypaxial–hypaxial type were chosen at random, and one optical section through the middle of these aggregates (i.e., maximum number of cell–cell contacts) was captured. For

each cell on the optical sections, the number of same-color (red–red, green–green) and opposite-color (red–green) contacts was counted. Subsequently, the average percentage of same- versus opposite-color contacts and the standard deviation was determined for each type of aggregate. The Student's *t* test was used to compare the percentage of same-color contacts in epaxial–hypaxial and control aggregates.

In situ hybridisation

Double whole-mount in situ hybridisation was carried out according to Dietrich et al. (1997, 1998), with a detergent mix (1% IGEPAL, 1% SDS, 0.5% deoxycholate, 50 mM Tris, pH 8, 1 mM EDTA and 150 mM NaCl) replacing ProteinaseK. Probes and their expression patterns are detailed in the following: *Alx4* (Takahashi et al., 1998); *En1* (Logan et al., 1992); *Noggin* (Hirsinger et al., 1997; Marcelle et al., 1997); *Paraxis* (Šošic et al., 1997); *Pax3* (Goulding et al., 1994); *Shh* (Johnson et al., 1994); *Sim1* (Pourquié et al., 1996); *Wnt5b* (Cauthen et al., 2001); and *Wnt11* (Tanda et al., 1995).

Sectioning

Embryos were embedded in 20% gelatin at 4°C, fixed in 4% PFA and cross sectioned to 50 μm on a Pelco 1000 Vibratome.

Photomicroscopy

After in situ hybridisation, embryos or tissue fragments were cleared in 80% glycerol or PBS. To improve the visibility of somitic expression pattern, whole embryos were split midsagittally. To photograph whole somites in detail, also the neural tube was removed. Embryos, somite preparations and sections were photographed on a Zeiss Axioskop, using fluorescence or Nomarski optics. Optical sections of cell aggregates were generated using a Leica SP1 confocal scanning microscope.

Results

Comparative expression analysis of En1, Sim1 and Alx4 in the avian somite

The amniote dermomyotome gives rise to the dorsal dermis and to distinct epaxial and hypaxial skeletal muscles, which in the adult are separated by a distinct connective tissue sheet (septum laterale; Christ and Ordahl, 1995; Goodrich, 1958; Gossler and Hrabe de Angelis, 1998). In the early embryo, however, epaxial–hypaxial dermomyotome and myotome are morphologically continuous. Nevertheless, a horizontal subdivision has been suggested for them, based on the expression patterns of the homeobox containing transcription factor En1, the basic helix-loop-helix transcription factor Sim1, and the homeobox containing transcription factor Alx4 (Ikeya and Takada, 1998; Spörle, 2001; Takahashi et al., 1998). Confusingly, *En1* has been suggested as a dermomyotomal marker, or as a marker for the central "intercalated" myotome, or as a marker for a subset of dermal precursors (Davis et al., 1991; Gardner and Barald, 1992; Ikeya and Takada, 1998; Logan et al., 1992; Olivera-Martinez et al., 2002; Spörle, 2001; Wurst et al., 1994). *Sim1* is generally accepted as a marker for the lateral somite half (dermomyotome, myotome and sclerotome) and hence a marker for hypaxial programmes (Pourquié et al., 1996) but has also been suggested as further marker for the "intercalated" myotome (Spörle, 2001). Finally, also *Alx4* has been suggested as central marker, restricted however to the dermomyotome (low levels of expression are also found in the sclerotome; Takahashi et al., 1998). To ascertain sites of expression and to associate expression domains with epaxial–hypaxial programmes, we reinvestigated the expression patterns of *En1*, *Sim1* and *Alx4* in the chick embryo from embryonic day E2½ (HH16) to E5 (HH27), using whole-mount in situ hybridisation and vibratome sectioning (Fig. 1 and data not shown). In double labelling experiments, the paired and homeobox containing transcription factor *Pax3* was used to mark the dermomyotome as a whole and in particular, to highlight the dorsomedial and ventrolateral dermomyotomal lips (dml, vll; Goulding et al., 1994).

Our analysis revealed that avian *En1* expression commences in dorsoventrally differentiated somites with the developmental ages 8–10 (shown for E3/HH20 in Fig. 1A, arrowhead), in line with Olivera-Martinez et al., 2002. The initial staining resides in a medial territory of the somite and is confined to the dermomyotome (Figs. 1A, B and E). The *En1* signal abuts the elevated *Pax3* signal in the dml but leaves a gap to the strong *Pax3* signal in the vll (Fig. 1E, red staining). This gap is occupied by the *Sim1* signal, which directly abuts the expression domain of *En1* (Figs. 1C and F; note that *Sim1* expression is down-regulated in the vll at this stage). *Alx4* incorporates the expression domains of *En1* plus *Sim1*, omitting however the strongly *Pax3*-expressing lips (Figs. 1D and G). Thus, we can confirm *Alx4* as a central dermomyotomal marker, pointing at processes shared between the epaxial and hypaxial domains. *En1* and *Sim1*, however, do not label the whole central dermomyotome but molecularly subdivide it in a horizontal plane.

Comparing anterior (i.e., mature) and posterior (i.e., immature) somites at HH20 (Fig. 1A) or comparing the flank somites at HH20 and HH24 (Figs. 1B and H), it becomes obvious that during development, the *En1* domain elongates considerably in dorsomedial–ventrolateral direction. From maturation stage XX onwards, *En1* expression begins in the myotome in cells that belong to the late arriving population of myoblasts, which enter from the rostral and caudal dermomyotomal lips (Kahane et al., 2001;

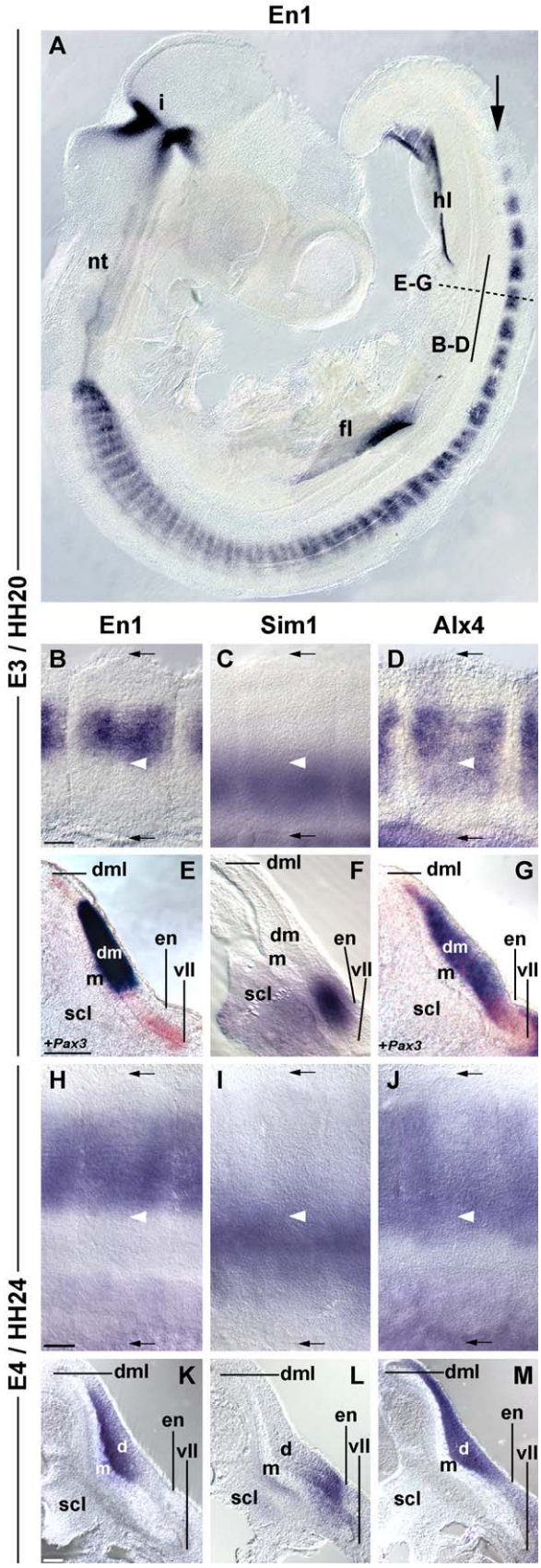

L. Cheng and S. Dietrich, unpublished observations). Furthermore, *En1* expression is maintained in the deep-ithelialising dermal precursors, such that flank somites at HH24, for example, show aligned expression domains for *En1* in a subdomain of myotome and prospective dermis (dermatome; Fig. 1K; see also Olivera-Martinez et al., 2002). Importantly, the *En1* signals still abut the *Sim1* signals that label the lateral aspect of myotome and dermatome (compare Figs. 1H–I and K–L). *Alx4* remains confined to the dermatome, here encompassing the expression domains of *En1* and *Sim1* as before (Figs. 1J and M). Thus, *Alx4* labels all the somitic cells destined to contribute to the dermis. In contrast, *En1* and *Sim1* expressions are not associated with a particular path of cellular differentiation. Rather, *En1* and *Sim1* maintain the molecular subdivision of the somite as their expression is superimposed onto myotome and dermatome.

Fig. 1. Comparative expression analysis of En1, Sim1 and Alx4. (A–G) Embryos at E3/HH20. (A) Lateral view of a whole embryo stained for *En1*, anterior is in the top left corner. *En1* is expressed in the developing isthmus (i), the V1 interneurons in the neural tube (nt) and the ventral limb ectoderm (fl, hl). Somitic *En1* expression commences in somites VIII–X and is confined to a central territory (arrow). In more mature somites further anterior, the signals expand mediolaterally, in line with somite outgrowth. (B–D) Dorsolateral views of single flank somites (position indicated in A; dorsomedial to the top, anterior to the right), stained for *En1* (B), *Sim1* (C) and *Alx4* (D). The dorsomedial and ventrolateral borders of the somites are indicated by arrows. Note that the *En1* domain abuts the *Sim1* domain (*Sim1* expression borders less obvious due to overlying expression in dermomyotome, myotome and sclerotome; see F), and both are encompassed in the *Alx4* domain. The border of *En1*/*Sim1* expression is indicated by an arrowhead and plotted onto the *Alx4* territory. (E–G) Cross sections of flank somites as indicated in A; dorsal to the top, medial to the left. (E) *En1* staining in blue and *Pax3* staining in red. Note that *En1* expression is confined to the dermomyotome, abutting the *Pax3* signal in the dml, but not reaching the *Pax3* staining in the vll. (F) *Sim1* staining. Note that *Sim1* expression labels the lateral aspect of dermomyotome, myotome and sclerotome in the dermomyotome abutting the *En1* signals. Also note that *Sim1* expression is down-regulated in the vll. (G) *Alx4* staining in blue and *Pax3* staining in red. *Alx4* labels both the *En1* and *Sim1* domains in the dermomyotome, omitting the dml and vll. Note that the lateral border of the *Alx4* zone is demarcated by the ectodermal notch (en). (H–M) Embryos at E4/HH24. (H–J) Dorsolateral views of flank somites, same magnification and orientation as in (B–D). Note the elongation of the somite; in particular, the *En1* (H) and *Alx4* domains (J) have expanded in dorsomedial–ventrolateral direction. The *En1* (H) and *Sim1* domains (I) still abut and are enclosed in the *Alx4* domain (J). Demarcation of somite and expression borders as in (B–D). (K–M) Cross sections of flank somites, same orientation, but lower magnification as (E–G). (K) *En1* expression. Note that *En1* expression labels a subterritory of the myotome and the deepithelialised dermal precursors (dermatome, d). (L) *Sim1* expression, labelling the dermatome up to the ectodermal notch, the lateral myotome and the lateral sclerotome. Note that in dermatome and myotome, *En1* and *Sim1* signals abut. (M) Somitic *Alx4* expression is confined to the dermatome, here encompassing the *En1* and *Sim1* domains as before. Lateral to the ectodermal notch, weaker *Alx4* staining labels the lateral mesoderm. Abbreviations: en, ectodermal notch; d, dermatome; dm, dermomyotome; dml, dorsomedial dermomyotomal lip; fl, fore limb; hl, hind limb; I, isthmus; m, myotome; nt, neural tube; scl, sclerotome; vll, ventrolateral dermomyotomal lip. The scale bars in B and H represent 50 μm for B–D and H–J, the scale bar in E represents 50 μm for E–G and the scale bar in K represent 50 μm for K–M.

Origin and distribution of En1 cells

The expression of *En1* medially adjacent to the *Sim1* domain suggests that *En1* cells may be part of the epaxial programmes of the somite. However, the signals reside at a distance to the axial midline and eventually occupy a wide mediolateral extent of the dermomyotome. Although the expansion of the *En1* domain is in line with somite outgrowth (Ben-Yair et al., 2003), it cannot be excluded that hypaxial cells are added on to this domain, casting doubt on the reliability of *En1* as epaxial marker. To investigate where the *En1*-expressing cells are born and how they reach their final position, we performed two series of experiments: (a) vital labelling of somites stages I, II, V and X with the fluorescent dyes DiI and DiO (Fig. 2), and (b) orthotopic grafting of thirds, halves or two thirds of quail segmental plates into chick hosts (Fig. 3).

DiI–DiO labelling

The dorsomedial quadrant of the somite is the source of cells for the epaxial myotome; recent studies also suggested it as source of the epaxial dermomyotome or dermatome (Denetclaw et al., 1997; Huang and Christ, 2000; Kahane et al., 1998a; Ordahl et al., 2001). Hypaxial cells on the other hand are thought to stem from the lateral somite half (Cinnamon et al., 1999; Denetclaw and Ordahl, 2000; Huang and Christ, 2000; Ordahl and Le Douarin, 1992). To locate the initial boundary between both programmes and to trace the origin of the *En1* cells, we, at HH14, labelled a small group of cells in the dorsomedial wall of the recently formed somites I and II with DiI and a second group of cells in the dorsal centre of the same somites with DiO (n = 27; Figs. 2A and B). We then reincubated the embryos for 24 h, allowing the labelled somites to reach the developmental ages XVI–XVII, and photographed the distribution of the dyes (shown for somite II in Fig. 2C). Subsequently, the embryos were bisected, the labelled somites were analysed for the expression of *En1* (Fig. 2D) and the corresponding somites on the contralateral side (symmetrical to the labelled somites) for the expression of *Sim1* (Fig. 2E). We rephotographed the somites such that the sites of fluorescence and marker gene expression could be compared. We found that the DiI- and DiO-labelled cells retained their relative mediolateral position and did not mix (Fig. 2C). Importantly, the DiI-labelled cells contributed to the *En1* expression domain, while the DiO-labelled cells had been displaced laterally and contributed to the expression domain of *Sim1* (DiI = red and DiO = green arrowheads in Figs. 2D and E). This suggests that the initial epaxial–hypaxial boundary lies medial to the dorsal centre of a newly formed somite, consistent with the lateral boundary of *Sim1* expression at this stage (Dietrich et al., 1998). It furthermore suggests that *En1* cells belong to the epaxial programme as they originate from the medial wall of the somite.

When we cultured the labelled embryos for only 7–8 h, that is, until the labelled somites had reached stages V–VI, we noticed that the DiI-stained cells occupied the medial half of the dermomyotome, indicating that the somite had rotated laterally and the dorsomedial quadrant of the somite had begun outgrowth (not shown). To determine whether within this area, it was the dorsomedial lip or the adjacent dermomyotome proper that delivers cells into the *En1* domain, we injected DiI into the dml and DiO into the adjacent epaxial portion of the dermomyotome of somite V at HH14 (n = 17; Figs. 2F and G). The embryos were again cultured for 24 h, allowing the labelled somites to reach stage XX and processed as before (Figs. 2H–J). We found that from both injected sites, labelled cells had contributed to the *En1* domain but remained outside of the *Sim1* territory.

To investigate the mechanism that leads to the mediolateral expansion of the *En1* zone during somite outgrowth, we injected DiI into the dorsomedial lip and DiO into the *En1* domain of stage X somites at HH14, that is, somites that just had begun *En1* expression (n = 26; Figs. 2K and L). The embryos were cultured for 24 h until the injected somites had reached stage XXV (Figs. 2M–O). As at stage V, the labelled cells contributed to the *En1*, but not the *Sim1* domain. This suggest that cell proliferation in situ as well as addition of cells from the dml drive the outgrowth of the epaxial dermomyotome and the expansion of the *En1* expression domain.

Orthotopic grafting of third, half or two third segmental plates

Our labelling experiments suggested that *En1* precursor cells originate from the dorsomedial wall of the newly formed somite. To confirm this finding, we used a further, independent method, the orthotopic quail-chick grafting technique. Unfortunately, dermomyotomal grafts or grafts from epithelial somites frequently fail to liaise with the cut edges of the host somite (unpublished observations). On the other hand, the segmental plate is a compact tissue with little cell movement (Palmeirim et al., 1997). Thus, grafting of longitudinally split segmental plates will lead to the same results as the more artefact-prone grafting of epithelial somite fragments. We therefore excised the medial third or the medial half or the lateral half or two thirds of the right chick segmental plate at HH11-12 and replaced it with the corresponding tissue from a stage-matched quail donor. The embryos were reincubated for 40 h in order to allow even the posterior segmental plate to reach an *En1*-expressing state. Subsequently, the embryos were double labelled to compare the position of *En1* signals and the QCPN-stained quail cells. The results of the operations are summarised in Table 1.

We found that when medial third-segmental plates were grafted as outlined in Fig. 3A, the medial dermomyotome, myotome and sclerotome were quail-derived (n = 2; Figs. 3B and C). Significantly, the lateral border of the *En1* expression domain (Fig. 3C, blue arrowhead) coincided with the lateral extent of QCPN-stained quail cells (Fig. 3C,

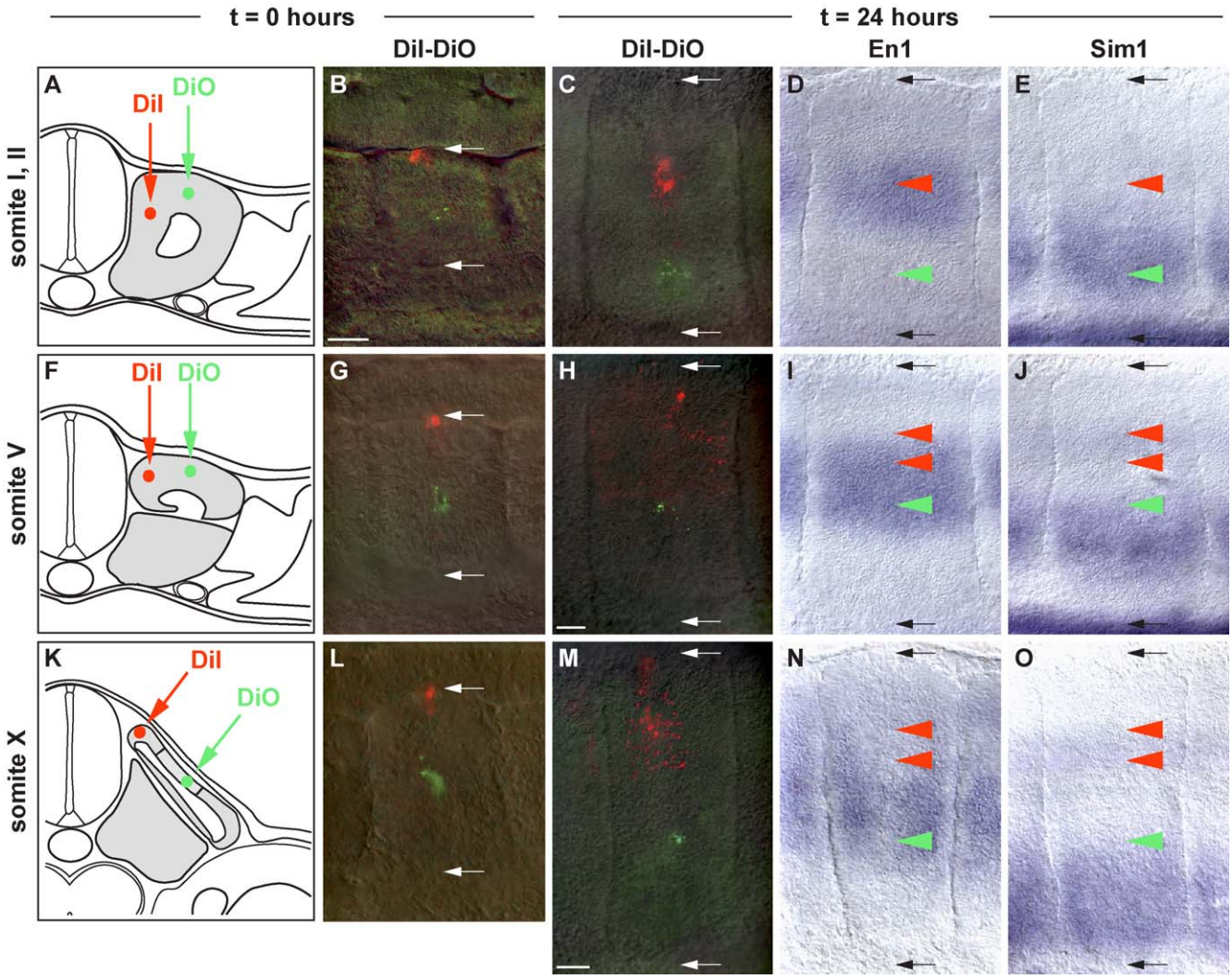

Fig. 2. Origin and distribution of *En1*-expressing cells mapped by DiI–DiO labelling. (A, F and K) Schematic cross sections indicating the time and sites of DiI (red) and DiO (green) labellings. (B, G and L) Dorsolateral views onto somites II (B), V (G) and X (L) at the time of labelling, dorsomedial to the top, anterior to the right. (C, H and M) Dorsolateral views of somites II, V and X 24 h after labelling, orientation as in B, G and L). (D, I and N) Dorsolateral views of the somites shown in C, H and M) after in situ hybridisation for *En1*; orientation as before. (E, J and O) Dorsolateral views of the somites opposite to C/D, H/I and M/N after in situ hybridisation for *Sim1*; orientation as before. The arrows in B–E, G–J and L–M indicate the dorsomedial and ventrolateral borders of the somite. The scale bar in B represents 50 μm for B–E, G and L, the scale bar in H represent 50 μm for H–J and the scale bar in M represent 50 μm for M–O. (A–E) When recently formed somites I–II were labelled as schematised in A and shown for somite II in B, then 24 h later (C; also somite II labelling), the cells originating from the medial wall of the somite (DiI, red) were located in a central position within the dermomyotome, while cells originating from the middle of the dorsal somitic wall (DiO, green) were displaced laterally. The DiI-labelled cells resided within the *En1* domain (D, red arrowhead), the DiO-labelled cells lateral to it (green arrowhead). Plotting the distribution of the dyes onto the corresponding somite of the controlateral side (E), it appears that the DiO-stained cells reside in the area of *Sim1* expression. (F–J) When in a stage V somite, the dorsomedial lip was DiI (red) labelled and the dorsal centre of the dermomyotome with DiO (green; F,G), then 24 h later, both sites were located in a more central position H and had contributed to the expression domain of *En1* (I, arrowheads). Plotting the distribution of the dyes onto the corresponding somite of the controlateral side (J), it appears that the cells did not contribute to the *Sim1* domain. (K–O) Labelling of a stage X dermomyotome with DiI (K and L, red) applied to the dorsomedial lip and DiO (K and L, green) to the dermomyotomal centre. Note that in somites of this stage, *En1* is expressed at the location indicated in yellow in (K). After 24 h, the labelled cells occupied a more central position (M) and had contributed to the *En1* domain (N, arrowheads). Plotting the sites of DiI–DiO staining onto the corresponding somite on the opposite side of the embryo as before, it appears that *Sim1* cells were not labelled.

brown arrowhead). When half segmental plates were grafted (n = 3; Figs. 3D–F), the QCPN staining laterally exceeded the *En1* domain (note distance of blue and brown arrowhead in Fig. 3F). When lateral two third segmental plates were exchanged (n = 4; Figs. 3G–I), the QCPN staining occupied the lateral dermomyotome, myotome and sclerotome, reaching up to the *En1* domain, while lateral half segmental plate grafts left a gap to the *En1* expression domain (n = 2, not shown). These observations confirm that the cells destined to express *En1* stem from the medial wall of the somite.

To test whether the expansion of the *En1* domain that occurs between HH20 and 24 is due to growth within the *En1* domain as suggested by the DiI–DiO labellings, or instead by the incorporation of formerly *Sim1*-expressing

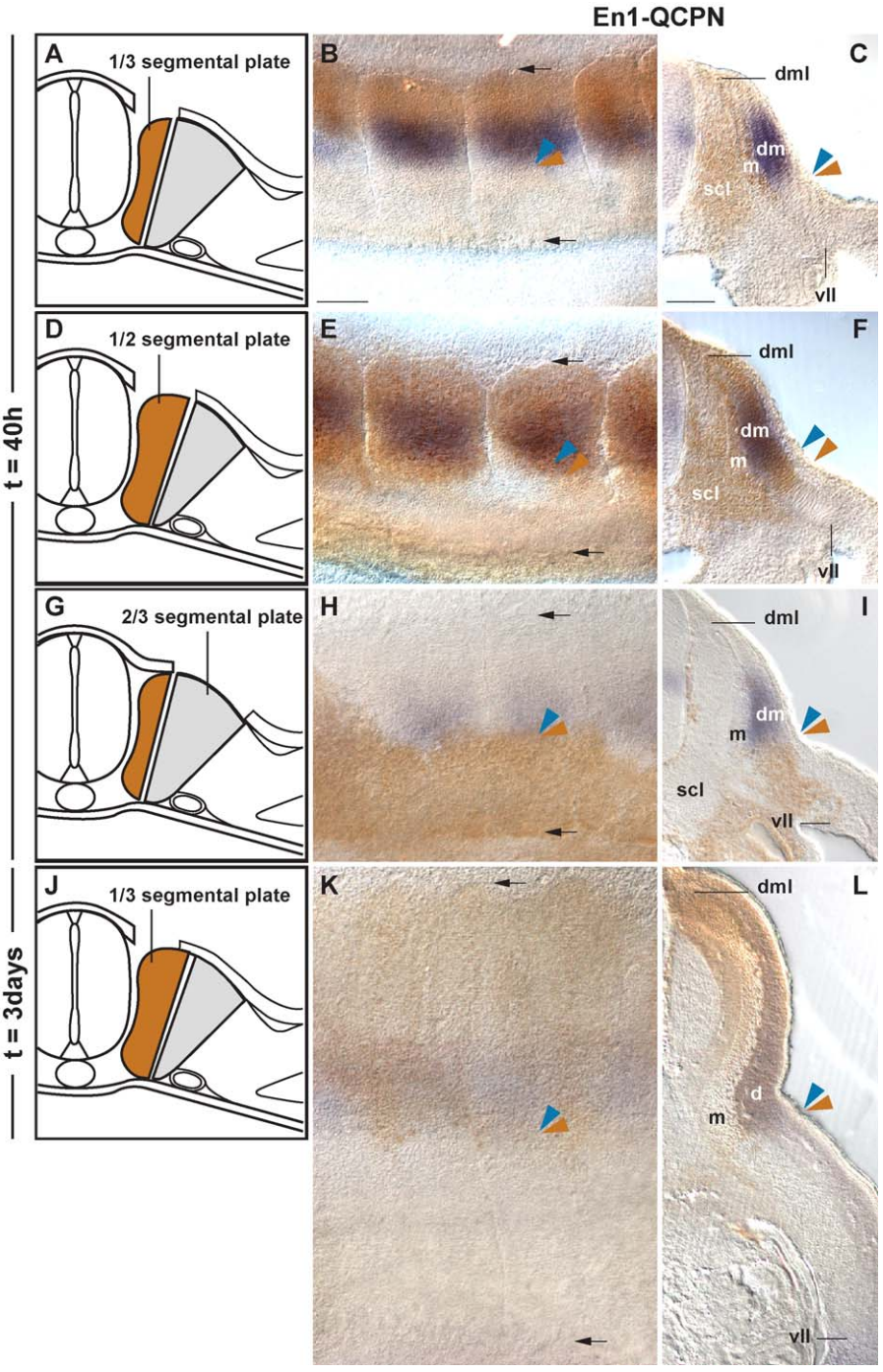

Fig. 3. Origin and distribution of *En1* cells mapped by orthotopic quail-chick grafting of third segmental plates (A–C, J–L), half-segmental plates (D–F) and two third segmental plates (G–I). (A, D, G and J) Schemes of operation, quail-derived grafts labelled in brown; time of reincubation is indicated. (B, C, E, F, H, I, K and L) Embryos stained for *En1* expression in blue and quail cells in brown (QCPN antibody), with (B, E, H and K) dorsolateral views (dorsomedial to the top, anterior to the right; the somitic borders are indicated by arrows) and (C, F, I and L) cross sections (dorsal to the top, medial to the left). (A–C) When medial third-segmental plates were grafted, the lateral extent of quail cells and the lateral border of *En1* expression coincided (brown and blue arrowheads in C). (D–F) When medial half-segmental plates were grafted, the QCPN staining demarcating the quail cells laterally exceed the *En1* domain (F, distance of brown and blue arrowheads). (G–I) When lateral two third segmental plates were grafted, the quail cells reached up to the lateral boundary of *En1* expression. (J–L) When embryos that received medial third-segmental plate grafts were cultured for 3 days to E41/2, the lateral extent of quail cells still coincided with the lateral border of *En1* expression, indicating that the expansion of the *En1* domain during development is due to the growth of the *En1*-expressing somite territory, not the switch of expression profiles. The scale bar in B represents 100 μm for B and E; the scale bar in C represent 50 μm for C and F. Abbreviations as in Fig. 1.

Table 1
Summary of DiI–DiO labelling and chick-quail grafting

Experiment	Result
DiI labelling of dorsomedial wall of somites I and II; 24 h incubation (27)	Labelled cells in *En1* domain
DiO labelling of dorsal centre of somites I and II; 24 h incubation (27)	Labelled cells in *Sim1* domain
DiI labelling of dml of somite V; 24 h incubation (17)	Labelled cells at medial edge of *En1* domain
DiO labelling of dermomyotomal centre of somite V; 24 h incubation (17)	Labelled cells at lateral edge of *En1* domain
DiI labelling of dml of somite X; 24 h incubation (26)	Labelled cells at medial edge of *En1* domain
DiO labelling of the *En1*-expressing area of the dermomyotome; somite X, 24 h incubation (26)	Labelled cells within *En1* domain
Orthotopic grafting of medial 1/3 segmental plate; 40 h and 3 days incubation	Lateral border of QCPN and *En1* staining coincide (5)
Orthotopic grafting of medial 1/2 segmental plate; 40 h incubation	QCPN staining exceeds *En1* staining and reaches ectodermal notch (3)
Orthotopic grafting of lateral 1/2 segmental plate; 40 h incubation	Complementary to medial 1/2 segmental plate grafting (2)
Orthotopic grafting of lateral 2/3 segmental plate; 40 h incubation	Complementary to medial 1/3 segmental plate grafting (4)

The number of experimental embryos is given in parentheses. Note that the contribution of dye-labelled or quail-derived cells to tissues other than the dermomyotome is not listed. Abbreviations as in Figs. 1 and 2.

cells, we performed orthotopic grafting of medial-third segmental plates, this time incubating the embryos for 3 days to reach HH24 (n = 3; Figs. 3J–L). Notably, the lateral extent of QCPN staining coincided with the lateral border of *En1* expression, underlining that during dermomyotomal outgrowth, *En1* expression remains confined to the cells of medial or epaxial descent.

Control of En1 expression

The site of *En1* expression medial to the *Sim1* domain and the origin of *En1* cells from the medial somite wall place *En1* into the epaxial programmes of the somite. However, *En1* expression occurs late and far from the axial midline tissue, notochord and neural tube, known to control the development of medial or epaxial somite derivatives (reviewed by Brent and Tabin, 2002). This suggests that *En1* expression is controlled by a complex regulatory mechanism. To decipher these regulatory cascades, we systematically manipulated the structures surrounding the chick paraxial mesoderm by in ovo microsurgery. In detail, we (a) ablated notochord plus neural tube or notochord plus floor plate and replaced the latter by Shh-loaded beads (Figs. 4C–F); we (b) ablated the dorsal neural tube and replaced it by different types of Wnt-expressing cells (Figs. 4G–K); we (c) removed the surface ectoderm, also replacing it by Wnt-expressing cells (Figs. 4L–P); we (d) removed the lateral plate mesoderm and replaced it by BMP4-loaded beads (Fig. 5); and finally, we (e) rearranged the position of the tissues we found to positively regulate *En1* expression to test for the mode and timing of their signalling (Fig. 6).

To test for the formation of *En1* precursor cells, operations were performed at the level of the segmental plate at HH12–13 (HH11–12 for the neural tube rotations),

Fig. 4. Signals positively regulating *En1* expression. (A_i–P_i) Schematic cross sections indicating the microsurgical procedures, dorsal is to the top. Notochord, floor plate and Shh bead are depicted in orange, dorsal neural tube and Wnt1-expressing cells in turquoise, surface ectoderm and Wnt6 cells in dark blue and intermediate and lateral mesoderm in red. (A_{ii}–P_{ii}) Cross sections of embryos 24 h postsurgery (operation at segmental plate or somite V levels, A_{ii}–G_{ii}, I_{ii}–L_{ii}, N_{ii}–P_{ii}) or 16 h postsurgery (operation at somite X levels, B_{ii}, H_{ii}, M_{ii}), stained for *En1*/blue and *Pax3*/red (A_{ii}–E_{ii}, G_{ii}–H_{ii}, L_{ii}–M_{ii}) or for *En1*/blue only (F_{ii}, I_{ii}–K_{ii}, N_{ii}–P_{ii}); dorsal is to the top. (A) Unoperated control for operations at segmental plate levels, (B) unoperated control for operations at the levels of somite V or X. Note the *En1* domain in the dermomyotome next to the elevated *Pax3* staining in the dml, but distant from the elevated *Pax3* signal in the vll. (C) Ablation of the axial midline tissues, neural tube and notochord, at the level of the segmental plate, that is, before the specification of epaxial dermomyotomal or myotomal precursors. *En1* fails to be expressed, elevated *Pax3* signals encompass the whole somite (arrows). (D) Ablation of notochord and floor plate at the level of the segmental plate prevents *En1* expression both in the somite (arrows) and in the neural tube, while *Pax3* signals are ventromedially expanded. (E) Ablation of notochord and floor plate at somite stage V, that is, after the first *En1* precursor cells reached their final location, but before the onset of *En1*. Note that the expression of *En1* (arrows) and *Pax3* is unaffected. (F) Ablation of notochord or floor plate at the level of segmental plate, followed by the insertion of a Shh-loaded bead in place of the absent ventral structures. Shh restores the expression of *En1* both in the somite (arrows) and in the neural tube. (G) Unilateral ablation of the dorsal neural tube at segmental plate levels prevents *En1* expression on the operated side (arrow). (H) Unilateral ablation of the dorsal neural tube at somite X levels prevents *Pax3* expression in the dml (arrowhead), but *En1* expression is unaffected (arrow). (I) Unilateral ablation of the dorsal neural tube at segmental plate levels, followed by insertion of Celltracker Orange-stained RatB1a control cells. Note that *En1* expression fails on the operated side (arrow). (J) Unilateral ablation of the dorsal neural tube at segmental plate levels and insertion of RatB1a cells expressing Wnt1. Note that *En1* is expressed (arrow). (K) Unilateral dorsal neural tube ablation followed by the insertion of cells expressing Wnt6; no rescue of *En1* expression (arrow). (L) Separation of paraxial mesoderm and overlying ectoderm by tantalum foil at segmental plate levels; the position of the foil is indicated. Note that *En1* expression is prevented on the operated side (arrow). (M) Separation of the already *En1*-positive somite X from the surface ectoderm eliminates expression of *En1* (arrow). (N) Separation of paraxial mesoderm and ectoderm at segmental plate levels, followed by insertion of Celltracker Orange-stained RatB1a control cells underneath the tantalum foil. Note that *En1* expression is absent (arrow). (O) Separation of paraxial mesoderm and ectoderm and insertion of RatB1a cells expressing Wnt1. Note that *En1* expression is induced next to the graft (arrow). (P) Separation of paraxial mesoderm and ectoderm and insertion of RatB1a cells expressing Wnt6; no restoration of *En1* expression (arrow). Abbreviations: dnt, dorsal neural tube; ect, surface ectoderm; fp, floor plate; not, notochord; nt, neural tube; lat mes, lateral mesoderm; som, somite; sp, segmental plate; others as in Fig. 1. The scale bar in A_{ii} represents 100 μm in (A_{ii}–P_{ii}).

control (sp)
control (somV/X)
-not/nt (sp)
-not/fp (sp)
-not/fp (somV)
-not/fp +Shh (sp)
-dnt (sp)
-dnt (som X)
-dnt + control cells (sp)
-dnt + Wnt1 cells (sp)
-dnt + Wnt6 cells (sp)
-ect (sp)
-ect (som X)
-ect + control cells (sp)
-ect + Wnt1 cells (sp)
-ect + Wnt6 cells (sp)
En1
Pax3
Shh
ect
nt
not
lat mes
dm
m
scl
cells
control cells
Wnt1 cells
Wnt6 cells
foil
tantalum foil
En1 only

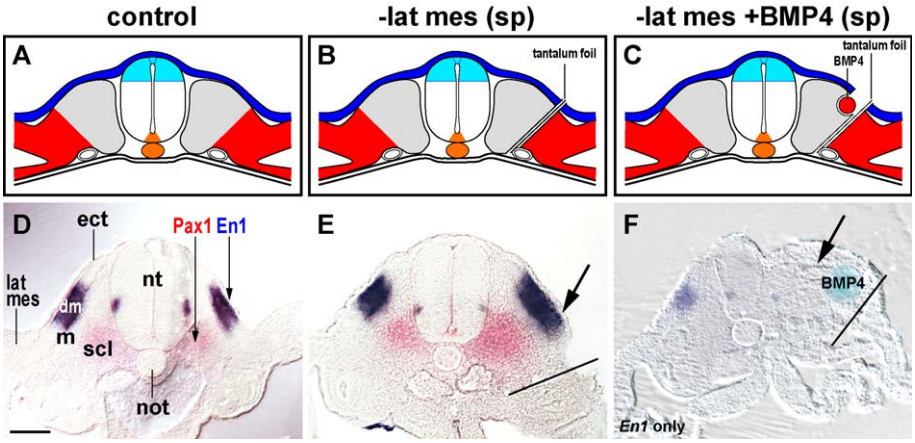

Fig. 5. Signals negatively regulating *En1* expression. (A–C) Schemes of operations (all performed at segmental plate levels), orientation and colour codes as before, BMP4 bead in red. (D and E) Cross sections stained for *En1*/blue and *Pax1*/red, or (F) for *En1* alone, all 24 h postsurgery, dorsal to the top. (D) Unoperated control, showing *En1* expression in the dermomyotome and *Pax1* expression in the medial sclerotome. (E) An insertion of tantalum foil between the paraxial and the intermediate plus lateral mesoderm causes the lateral expansion of the *Pax1* as well as the *En1* domain (arrow). (F) Insertion of foil between paraxial and intermediate or lateral mesoderm, followed by an implantation of a BMP4 bead (10 μg/ml) into the paraxial mesoderm next to the foil. Note that the bead overcompensated for the absence of lateral mesoderm-derived signals and wiped out the expression of *En1*. Abbreviations as in Figs. 1 and 4. The scale bar in D represents 100 μm in D–F.

that is, before cells in the medial wall of the somite are specified. The embryos were reincubated for 24 h to reach HH20. At this stage, the control embryos displayed robust expression of *En1* (blue staining; Figs. 4Aii, 5D and 6E). In addition, we performed the same operation/24-h reincubation at the level of somites V–VIII, that is, briefly before the onset of *En1* expression; and to test for *En1* maintenance, we operated at the level of somites XII–XV at HH13, that is, somites, which had reliably established *En1* expression. These embryos were reincubated for further 16 h. For operations at somite stages V and X, the mediolateral elongation of the *En1* domain was under way in controls (Fig. 4B_{ii}, blue staining). To control that the operations has the desired effect on somite patterning, *Pax3* (Figs. 4Aii–Eii, Gii–Hii, Lii–Mii, 6E–F) or *Pax1* expression (5D–E) was followed simultaneously (red staining). The result of all operations with respect to *En1* expression is summarised in Table 2; for additional markers, see the chapters below.

The role of the axial midline tissues, notochord and floor plate and Shh signalling

The medial wall of the avian somite yields the precursors for the epaxial myotome, which require the axial midline tissues, notochord and neural tube for their development (Dietrich et al., 1997; Münsterberg and Lassar, 1995; reviewed by Brent and Tabin, 2002). Ablating the midline tissues at the level of the segmental plate or newly formed somites, we found that *En1* expression was prevented, while *Pax3* and *Sim1* expressions were up-regulated throughout the somite (n = 11; Fig. 4C; Dietrich et al., 1998). To test which of the axial midline tissues may be required for *En1* expression, we began, removing the notochord and the in this context functionally equivalent floor plate at segmental plate levels of HH12–13 embryos as outlined in Fig. 4D_i (n = 15). This operation prohibits the development of ventral identities both in the somite and in the neural tube as monitored by the ventral expansion of *Pax3* expression (Dietrich et al., 1997; Fig. 4D_{ii}, red staining). Significantly, *En1* expression was also missing (absence of blue staining in Fig. 4D_{ii}, arrows). When the ablation of notochord or floor plate was performed at the level of somites V–VIII (n = 13) or XII–XV (n = 14), however, *En1* signals were unaffected (Fig. 4E and data not shown). This suggests that notochord or floor plate act during the formation of the *En1* precursor cells.

In vivo and in vitro, the function of notochord or floor plate in epaxial myogenesis is mimicked by the signalling molecule Sonic hedgehog (Shh; Borycki et al., 1998, 1999; Fan and Tessier-Lavigne, 1994; Münsterberg et al., 1995; reviewed by Brent and Tabin, 2002). Moreover, Shh is the signal that controls the formation of *Engrailed*-expressing cells in the zebrafish somite (Currie and Ingham, 1996; reviewed by Stickney et al., 2000). We therefore tested whether Shh could rescue the *En1* precursors in the chick somite upon notochord or floor plate ablation at segmental plate levels. For this purpose, Shh-loaded beads (500 μg/ml, n = 12; Fig. 4F) or control beads (n = 2, not shown) were implanted into the gap left by the ablation, and the embryos were cultured for 24 h as before. We found that the Shh beads, but not the control beads, restored the expression of *En1* both in the somite (Fig. 4F_{ii}, arrows) and in the neural tube. This infers that, as in the zebrafish, notochord and floor plate-derived Shh is essential for the formation of *En1* cells in the avian somite.

The role of dorsal neural tube and Wnt signalling

Studies on mouse mutants harbouring dorsal neural tube defects suggested that in amniotes, the dorsal neural tube is

required for the formation of the *En1*-expressing dermomyotome (Ikeya and Takada, 1998). However, a recent study in the chick suggested that the neural tube is dispensable (Olivera-Martinez et al., 2002). To clarify this point, we performed unilateral neural tube ablations at the level of the segmental plate (n = 16), somites V–VIII (n = 16) and somites XII–XV (n = 14) as schematically shown in Figs. 4G_i and H_i. As the cut edge of the neural tube failed to rejoin the contralateral roof plate, the neural tube remained dorsally open. Nevertheless, the left side of the embryo, linked to the intact half of the neural tube, displayed wild-type expression pattern for *En1* (Figs. 4G_{ii} and H_{ii}, blue staining) and *Pax3* (red staining) at all stages. On the operated side, the dermomyotome was significantly shortened and *En1* expression was lacking when the operation was performed at segmental plate levels of HH12–13 embryos (Fig. 4G_{ii}, arrow). Interestingly, when the same operation was performed at HH14–15, faint *En1* signals were present, reminiscent of the findings of Olivera-Martinez (2002). Similarly, upon operations at stages V–VIII (HH12–13), *En1* expression was detectable, although at reduced levels or in mediolaterally shortened domains (not shown). At stages XII–XV (HH12–13), while the dorsomedial dermomyotomal lip was missing as evidenced by the absence of *Pax3* staining (Fig. 4H_{ii}, arrowhead), *En1* expression was unaffected (arrow). This suggests that in the early embryo, the dorsal neural tube is involved in the establishment and the initial expansion of the *En1* precursor pool but is not required for the activation or maintenance of *En1* expression.

In the mouse, *En1* expression is lacking when *Wnt1* and *Wnt3a* functions are absent (Ikeya and Takada, 1998). To test for a similar role of Wnt factors in the chick, we unilaterally ablated the dorsal neural tube at segmental plate levels of HH12–13 embryos and implanted either control cells (n = 11) or cells expressing *Wnt1* (normally expressed in the dorsal neural tube; Hirsinger et al., 1997; Marcelle et al., 1997; n = 6), *Wnt5a/b* (expressed in the anterior segmental plate and dml; A. El-Hanfy and S. Dietrich, unpublished observations and Cauthen et al., 2001; n = 3), *Wnt6* (expressed throughout the surface ectoderm; Schubert et al., 2002; n = 6) or *Wnt7a* (expressed in the surface

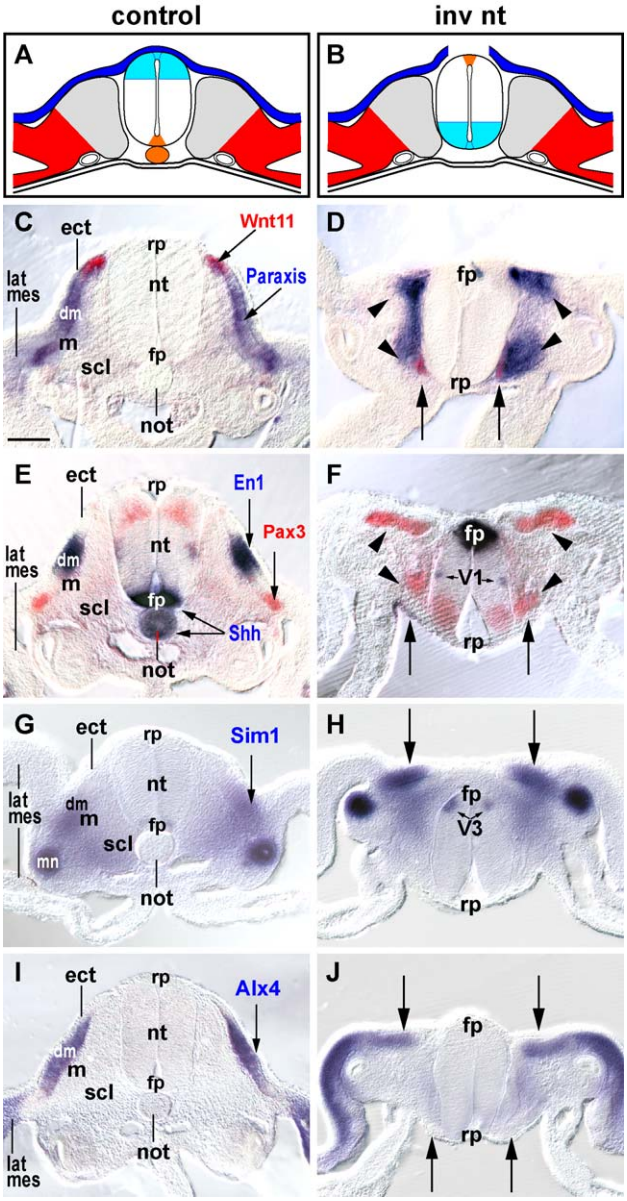

Fig. 6. Topology and sequence of *En1*-inducing signals. (A and B) Schematic cross sections delineating the procedure of dorsoventral neural tube inversion at the level of the segmental plate; colour code as in Fig. 4. (C–J) Cross sections of control (C, E, G and I) and operated embryos (D, F, H and J) 24 h after surgery; dorsal is to the top in all. (C and D) Cross sections, stained for *Paraxis* expression in the dermomyotome in blue and *Wnt11* expression in the dml in red. Note that following neural tube inversion, *Paraxis* is expressed both beneath the surface ectoderm and adjacent to the previously dorsal neural tube (D, arrowheads). *Wnt11* expression is confined to the *Paraxis*-expressing dermomyotomal epithelium next to the previously dorsal neural tube (arrows). This indicates that cells belonging to the epaxial programme reside in an ectopic, ventral location, distant from the surface ectoderm. (E and F) Cross sections showing *En1* expression in the dermomyotome in blue, *Shh* in notochord and floor plate also in blue and *Pax3* in the dermomyotome and dorsal neural tube in red. Upon dorsoventral inversion of the neural tube, *Pax3* expression continues in the previously dorsal neural tube, *Shh* expression in the original floor plate and *En1* expression in the V1 interneurons, suggesting the dorsoventral polarity of the neural tube remained unaltered. Note that *Pax3* expression labels the ventrally located, ectopic dermomyotome and the dorsally located dermomyotome underneath the surface ectoderm (arrowheads). *En1* expression fails, even in the ectopic epaxial dermomyotome (arrows), suggesting that after the specification of the epaxial precursor cells, ectodermal contact is needed for *En1* expression to be initiated. (G and H) *Sim1* staining. Note that upon neural tube inversion, while *Sim* expression in the V3 interneurons remains unaltered, expression in the dermomyotome underneath the surface ectoderm spreads to the midline, indicating its commitment to hypaxial programmes (arrows). (I and J) *Alx4* staining. At the operated site, *Alx4* expression is found in the dorsally located, *Sim1*-expressing, hypaxial dermomyotome (top arrows), not in the epaxial dermomyotome located in the ectopic ventral position (bottom arrows), suggesting that also *Alx4* expression depends on ectodermal signals. Abbreviations: inv, inverted; mn, mesonephros; rp, roof plate of the neural tube; others as in Figs. 1 and 4. The scale bar in I represent 100 μm in (C–J).

Table 2
Summary of ablation and heterotopic grafting experiments

Operation	Developmental age of paraxial mesoderm		
	Segmental plate	Somite V	Somite X
−nt/not	No *En1* (11)		
−not/fp	No *En1* (15)	Normal *En1* expression (13)	Normal *En1* expression (14)
−not/fp + BSA control beads	No *En1* (2)		
−not/fp + Shh (500 μg/ml)	Rescue of *En1* expression (12)		
−dnt	No *En1* (16)	No or reduced *En1* (16)	Normal *En1* expression (14)
−dnt + control cells	No *En1* (11)		
−dnt + Wnt1 cells	Rescue of *En1* expression (6)		
−dnt + Wnt5a/b cells	No *En1* (3)		
−dnt + Wnt6 cells	No *En1* (6)		
−dnt + Wnt7a cells	No *En1* (3)		
−ect	No *En1* (9)	No *En1* (6)	No *En1* (6)
−ect + control cells	No *En1* (4)		
−ect + Wnt1 cells	Rescue of *En1* expression (5)	Rescue of *En1* expression (5)	Rescue of *En1* expression (5)
−ect + Wnt5a/b cells	No *En1* (3)	No *En1* (3)	No *En1* (3)
−ect + Wnt6 cells	No *En1* (14)	No *En1* (14)	No *En1* (14)
−ect + Wnt7a cells	No *En1* (3)	No *En1* (3)	No *En1* (3)
−lat mes	Expanded *En1* (7)		
−lat mes + BSA control beads	Expanded *En1* (2)		
−lat mes + BMP4 100 μg/ml	*En1* expression lost (6)		
−lat mes + BMP4 10 μg/ml	*En1* expression lost (6)		
inv nt/fp	No *En1* (7; other markers 14)		

The number of operated embryos stained for *En1* expression is given in parentheses; for numbers of embryos stained with other markers, refer to text. Abbreviations as in Figs. 1, 4 and 6.

ectoderm overlying flank and limb somites; Yang and Niswander, 1995; $n = 3$). Prior to transplantation, the cells were tested for the expression of Wnt proteins (see Materials and methods). To facilitate the detection of the grafted cells, they were stained with Celltracker Orange (Figs. 4I_{ii}–K_{ii}, red staining). Neither the control cells (Fig. 4I) nor the cells expressing Wnt5a, 5b, 6 and 7a (Fig. 4K and not shown) rescued the expression of *En1* (blue staining). However, *Wnt1*-expressing cells reliably triggered *En1* expression (Fig. 4J, arrow).

The role of the surface ectoderm and Wnt signalling

The development of the dermomyotome has been shown to depend on signals from the surface ectoderm (Dietrich et al., 1997; Fan and Tessier-Lavigne, 1994; Šošic et al., 1997). A recent study proposed a role of the ectoderm also for the control of dermomyotomal *En1* expression (Olivera-Martinez et al., 2002). To address precisely when the *En1* precursor cells require the ectodermal signals to initiate *En1* transcription, we separated surface ectoderm and paraxial mesoderm at segmental plate levels ($n = 9$) and at the levels of somites V–VIII ($n = 6$) and XII–XV ($n = 6$) as described in Figs. 4L_i and M_i (Dietrich et al., 1997). As the ectoderm regenerates quickly, we inserted an impermeable barrier (tantalum foil) to permanently prevent ectodermal signalling. This operation has been shown to eliminate the expression of dermomyotomal markers in areas that do not receive compensatory signals from the neural tube (Dietrich et al., 1997). Importantly, the barrier prevented the *En1* expression at all times (Figs. 4L_{ii} and M_{ii}, blue staining). Thus, the surface ectoderm is required to initiate and maintain expression of the *En1* gene in the dermomyotome.

As Wnt genes have been suggested to carry out the signaling function of the surface ectoderm (Fan et al., 1997; Schubert et al., 2002; Tajbakhsh et al., 1998), we separated segmental plate plus somites V and XII from the surface ectoderm as described before, this time grafting (Celltracker Orange stained) control cells ($n = 4$) or cells expressing Wnt1 ($n = 5$), Wnt5a/b ($n = 3$), Wnt6 ($n = 14$) or Wnt7a ($n = 3$) underneath the foil. Control cells (Fig. 4N) and cells expressing Wnt6 (Fig. 4P) or Wnt5a/b and 7a (not shown) all failed to rescue the expression of *En1*. Interestingly, *En1* expression was restored when *Wnt1*-expressing cells were grafted (Fig. 4O). *Wnt1* is not expressed in the surface ectoderm, while its closest relative, *Wnt6*, is (Schubert et al., 2002). However, Wnt6 has only a limited signalling capacity (Fan et al., 1997), and in vivo seems to require cofactors provided by NIH3T3 cells (Schmidt et al., 2004) but not by RatB1a or DF1 cells (this study), demanding further functional studies on Wnt6. Nevertheless, our findings suggest that the surface ectoderm provides a Wnt1-like activity (i.e., signalling via the canonical pathway as reviewed by Miller, 2002) to trigger and maintain transcription of *En1*.

The role of the lateral plate mesoderm and BMP4

The lateral plate mesoderm, via BMP4, initiates the hypaxial programmes of the somite including the expression of *Sim1*, simultaneously repressing the epaxial networks

(Dietrich et al., 1998; Pourquié et al., 1996). It is therefore conceivable that the lateral mesoderm also negatively regulates the expression of *En1*. To test this possibility, we first separated the segmental plate from the intermediate and lateral mesoderm as described in Fig. 5B and Dietrich et al. (1998) ($n = 7$). This operation leads to an expansion of medial or epaxial somite markers such as the medial sclerotomal marker *Pax1* (Dietrich et al., 1998; Fig. 5E, red staining). Notably, *En1* expression was also expanded (Fig. 5E, blue staining, arrow).

Next, we separated segmental plate and intermediate or lateral mesoderm but inserted beads loaded with either 100 μg/ml ($n = 6$, not shown) or 10 μg/ml ($n = 6$; Figs. 5C and F) BMP4 or with BSA ($n = 2$, not shown). As BMP4 at 10 μg/ml up-regulates hypaxial somitic markers when added to the endogenous lateral plate-derived BMP4 (Dietrich et al., 1998), we expected that in absence of the lateral mesoderm, the BMP4-loaded beads would confine *En1* to its original expression domain. However, even at the lowest concentration, BMP4 overcompensated for the absence of the lateral plate mesoderm and wiped out the expression of *En1* (Fig. 5F, arrow) while control beads had no effect. This suggests that *En1* is extremely sensitive to BMP4, which negatively regulates the expression of the gene.

Sequential action of the En1-inducing signals

We showed that tissues that positively regulate *En1* expression are notochord or floor plate, dorsal neural tube and surface ectoderm. The operations at different stages of somite development suggested that notochord or floor plate and neural tube act on the *En1* precursors, while the subsequent transcriptional activation of *En1* is under ectodermal control. To obtain further proof for this scenario, we separated epaxial myotomal–dermomyotomal precursor cell formation from the transcriptional activation of *En1* by dorsoventrally inverting the axial midline tissues at segmental plate levels of HH11–12 embryos as described in Dietrich et al. (1997) and Fig. 6B. We reasoned that this operation would allow the completion of the first steps of epaxial dermomyotome–myotome development, namely, the neural tube or notochord-dependent specification of the precursors. However, as these cells reside in an unusual ventral position (Dietrich et al., 1997), the next step, the ectoderm-driven activation of *En1* should fail.

The manipulated embryos ($n = 21$) were incubated for 40 h to allow the somites in the operated region to reach a maturation age compatible with *En1* expression. Subsequently, the embryos were analysed for the dorsoventral organisation of the rotated neural tube (*Shh*, *Sim1*, *En1* and *Pax3*), the dorsoventral organisation of the somite (*Paraxis* and *Pax3*), the localisation of the dml (*Wnt11*, *Wnt5a/b* and *Noggin*) and the distribution of signals for *En1*, *Sim1* and *Alx4*. We found that the inverted neural tube had maintained its original dorsoventral organisation as monitored by *Shh* expression in the original floor plate (Fig. 6F, fp), *Pax3* expression in the alar plate (Fig. 6F, red staining next to the roof plate, rp), *Sim1* expression in the V3 interneurons next to the floor plate (Fig. 6H, V3) and *En1* expression in the V1 interneurons (Fig. 6F, V1; neuronal patterning reviewed by Goulding and Lamar, 2000). Accordingly, the somitic epithelium next to the previously dorsal, now ventral, neural tube expressed the dermomyotomal markers *Paraxis* (Fig. 6D, blue staining, lower arrowheads) and *Pax3*, (Fig. 6F, red staining, lower arrowheads) but also the dml markers *Wnt11* (Tanda et al., 1995; Fig. 6D, red staining, arrows) and *Wnt5a*, *Wnt5b* and *Noggin* (Cauthen et al., 2001; Hirsinger et al., 1997; Marcelle et al., 1997; not shown). This indicates that epaxial programmes were activated in this ectopic, ventral position. Conversely, the dermomyotomal epithelium located underneath the surface ectoderm expressed *Paraxis* (Fig. 6D, top arrowheads) and *Pax3* (Fig. 6F, top arrowheads), but in addition *Sim1* (Fig. 6H, arrows), indicating that in this position, hypaxial programmes unfolded. Importantly, none of the dermomyotomal epithelia expressed *En1*, not even the dermomyotome with epaxial marker gene expression (Fig. 6F, absence of blue staining in the somite, arrows). Likewise, this dermomyotome portion lacked expression of *Alx4* (Fig. 6J, bottom arrows), while the *Sim1*-expressing dermomyotome underneath the surface ectoderm succeeded to activate this gene (Fig. 6H, top arrows). Thus, the epaxial myotomal–dermomyotomal precursor cells, once specified, need to get under ectodermal control in order to activate expression of *En1* (and the epaxial expression of *Alx4*).

Sorting behaviour of En1 cells

Origin, expression profile and regulation of *En1* cells suggested that these cells are part of the epaxial somitic programmes (this study), while the laterally adjacent, *Sim1*-expressing cells are part of the hypaxial programmes (Pourquié et al., 1996). Our dye labelling and chick-quail grafting experiments, in line with the genetic studies in the mouse and lineage tracing in the chick (Eloy-Trinquet and Nicolas, 2002; Freitas et al., 2001; Selleck and Stern, 1991), furthermore suggested that epaxial and hypaxial cells do not trespass into the opposite territory. We therefore asked whether *En1*- and *Sim1*-expressing cells may set up a compartment boundary between them (i.e., imposing cell lineage restriction). Using a cell aggregation assay, Wizenmann and Lumsden (1997) have demonstrated that in the avian hindbrain, rhombomeres form compartment boundaries due to distinct adhesive properties of the cells on either side of the boundary: rhombomere cells sort by preferentially adhering to their own kind. We employed this assay to test for selective adhesion of epaxial and hypaxial cells in the dermomyotome; the experiment was repeated seven times.

In each experiment, approximately 200 stages X–XX dermomyotomes of HH20 embryos were isolated, cut horizontally where, based on our expression analyses, we expected the boundary between *En1* and *Sim1* signals to be positioned; then epaxial and hypaxial explants were collected separately (Fig. 7A). To control for the accuracy of our dissections, we embedded 8–10 of the explants in collagen and processed them for in situ hybridisation (Fig. 7B). We found that the epaxial explants expressed *En1* (Fig. 7C) but not *Sim1* (Fig. 7D), while the hypaxial portions lacked *En1* (Fig. 7E) but expressed *Sim1* (Fig. 7F). The remaining epaxial–hypaxial explants were labelled with either Celltracker Orange or Celltracker Green, then dissociated to obtain single cell suspensions and combined (Figs. 7G, J and M). Subsequently, the cell suspensions were incubated on a shaking platform for 4 h to allow the restoration of cell adhesion molecules and hence cell aggregation. The aggregates were then fixed and qualita-

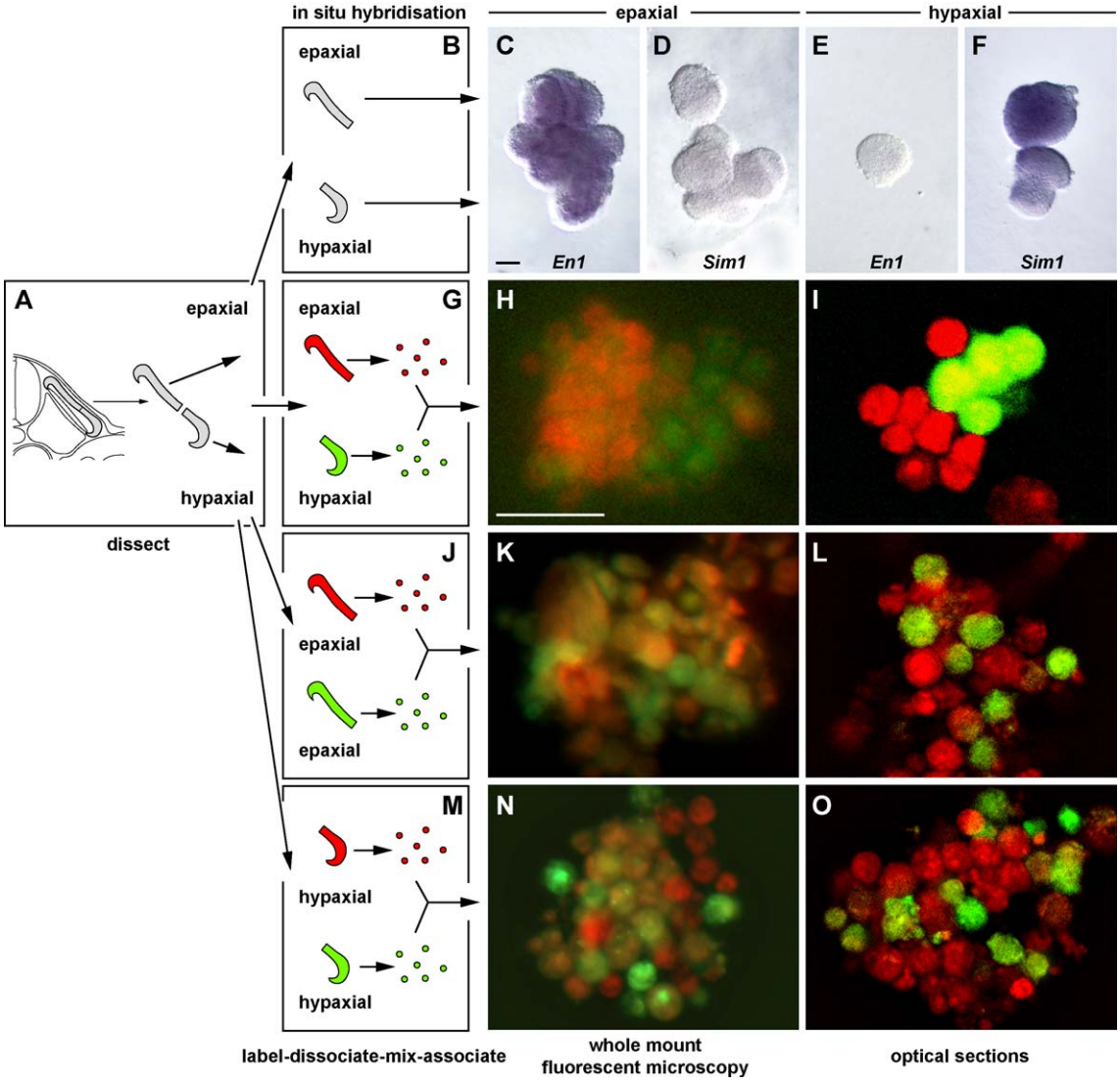

Fig. 7. Sorting behaviour of epaxial and hypaxial dermomyotome cells. (A, B, G, J and M) Schematic representation of the experimental procedures, encompassing dermomyotome isolation, separation of epaxial–hypaxial portions of the dermomyotome, then either in situ hybridisation of dermomyotome fragments with *En1* or *Sim1* probes (B), or fluorescent labelling of dermomyotome fragments, followed by tissue dissociation, cell mixing and 4 h of cell reassociation (G, J and M). (C–F) Nomarski images showing collagen-embedded dermomyotome fragments after in situ hybridisation; the scale bar in I represents 100 μm for (C–F). Note that the epaxial preparations express *En1* I, not *Sim1* (D); the hypaxial preparations lack *En1* (E) but express *Sim1* (F). (H, K and N) Compound fluorescent microscopy of whole aggregates and (I, L and O) confocal images presenting optical sections through aggregates, all 4 h after the mixing of the dissociated cells; the scale bar in (H) represents 25 μm for (H, I, K, L, N and O). (G–I) Aggregation of epaxial (red) plus hypaxial (green) cells. Note that epaxial and hypaxial cells preferentially adhered to their own kind as evidenced by the separate red and green staining. (J–L) Control aggregation of epaxial–epaxial cell preparations. The resulting aggregates consisted of freely distributed red and green cells, leading to yellow-orange staining in the whole-mount preparations due to overlapping green and red fluorescence (K) and interspersed red and green staining on the optical sections (L). (M–O) Control-aggregation of hypaxial–hypaxial cell preparations, resulting aggregates consist of randomly mixed cells.

tively and quantitatively analysed for the distribution of red and green cells using fluorescent microscopy (Figs. 7H, K and N) and confocal microscopy (Figs. 7I, L and O).

Due to the different size of epaxial and hypaxial dermomyotome fragments, more epaxial than hypaxial cells were available for the experiment. Thus, after having adjusted the volumes of the cells suspensions to standardise cell concentrations, we typically obtained 130 epaxial–hypaxial, 180 epaxial–epaxial and 90 hypaxial–hypaxial aggregates, each consisting of 40 (±13) cells (total number of cells was determined on series of optical sections of 40 randomly chosen aggregates). Significantly, both on whole-mount inspection (Fig. 7H) and on confocal sections (Fig. 7I), aggregates from epaxial–hypaxial preparations consisted of segregated red and green cell clumps. In contrast, aggregates from epaxial–epaxial (Figs. 7K and L) and hypaxial–hypaxial (Figs. 7N and O) preparations showed intermingling of red and green cells, suggesting that these cells mixed freely.

To quantify the extent of cell sorting or mixing, the number of same-colour (red–red, green–green) cell–cell contacts, which are homophilic for the epaxial–hypaxial aggregates, and the number of opposite-colour (red–green) cell–cell contacts that are heterophilic for the epaxial–hypaxial aggregates were counted on midaggregate optical sections of 20 epaxial–hypaxial, 20 epaxial–epaxial and 10 hypaxial–hypaxial aggregates containing on average 28 cells; a total of 1380 cells was analysed. We found that for epaxial–hypaxial aggregates, 70.46 ± 12.48% of the cell–cell contacts were same colour or homophilic, while for epaxial–epaxial and hypaxial–hypaxial, aggregates, same-colour contacts amounted to only 42.03 ± 12.71% and 36.91 ± 6.94%, respectively (Fig. 8). To establish the statistical significance of our findings, a Student's t test was performed, which provided a P value smaller than 0.0001 for the difference between epaxial–hypaxial and control aggregates. Thus, epaxial and hypaxial cells show a statistically significant sorting behaviour, preferentially adhering to their own kind. This suggests that in the somite, they may form a compartment boundary between them.

Discussion

In recent years, substantial progress has been made, identifying the regulatory cascades that initiate amniote epaxial and hypaxial myogenesis (reviewed by Brent and Tabin, 2002; Parkyn et al., 2002). However, the dermomyotome and subsequently the myotome and dermatome are morphologically continuous structures. Thus, the question must be asked as to how the epaxial and hypaxial precursor cells are segregated, how distinct, separately innervated epaxial and hypaxial muscles may form. The work presented here suggests that the expression domains of *En1* and *Sim1* molecularly define the epaxial–hypaxial interface. Moreover, our work suggests that *En1* and Sim1 cells may form a true compartment boundary, foreshadowing the point of epaxial–hypaxial subdivision of muscle.

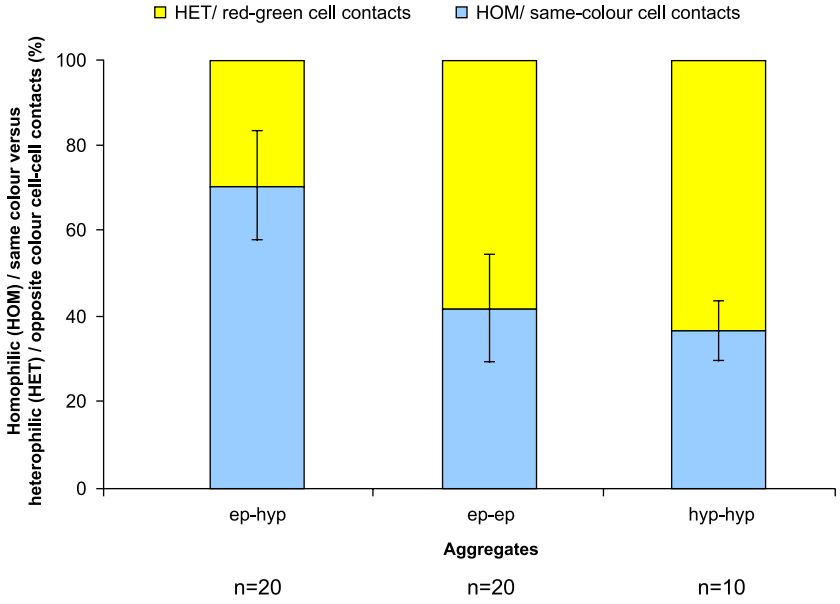

Fig. 8. Quantitative analysis of homophilic or same colour (blue) versus heterophilic or opposite colour (yellow) cell–cell contacts in midaggregate optical sections of epaxial–hypaxial (ep-hyp; n = 20), epaxial–epaxial (ep-ep; n = 20) and hypaxial–hypaxial (hyp-hyp; n = 10) cell aggregates. Values (%) are means ± SD. Note that for the epaxial–hypaxial aggregates, almost three quarters of the cell–cell contacts are homophilic; while for the control aggregates, same-colour interaction is significantly lower (P < 0.0001). This supports the hypothesis of cell sorting for epaxial–hypaxial cells, while cells of the same kind freely mix.

En1 and Sim1 molecularly subdivide the central dermomyotome, myotome and dermatome

Recent studies suggested that the amniote dermomyotome and myotome are horizontally subdivided, owing to the regionalised expression of markers such as *En1*, *Sim1* or *Alx4* (Davis et al., 1991; Gardner and Barald, 1992; Ikeya and Takada, 1998; Logan et al., 1992; Olivera-Martinez et al., 2002; Pourquié et al., 1996; Spörle, 2001; Takahashi et al., 1998; Wurst et al., 1994). However, these studies disagree on the precise sites of marker gene expression; some see *En1*, *Sim1* and *Alx4* as markers for the central or "intercalated" dermomyotome and myotome (Ikeya and Takada, 1998; Spörle et al., 2001; Takahashi et al., 1998), others refer to *Sim1* as a strictly lateral or hypaxial marker (Pourquié et al., 1996). Since the expression of markers may change over time thus leading to conflicting interpretations, we comparatively analysed the expression of the three markers in the thick embryo from E2 1/2 to E5 of development. Our study shows that *Alx4* is indeed a central dermomyotomal marker, labelling the dermomyotome proper and omitting the dorsomedial and ventrolateral dermomyotomal lips. *En1* and *Sim1* in contrast only label subdomains within the *Alx4* territory, with *En1* signals located medially, *Sim1* signals located laterally, and both markers abutting each other in the middle.

When the rostrocaudal dermomyotomal lips begin to deliver the late wave of myoblasts (Kahane et al., 2001) and the dermomyotome proper deepithelialises to form the dermatome (Christ et al., 1983), *En1* and *Sim1* expressions are maintained in the descendants of their respective expression domains. *Alx4* expression continues only in the dermatome, here however encompassing the *En1* and *Sim1* domains as before. Thus, *Alx4* expression is associated with the dermal fate of cells in the central dermomyotome. *En1* and *Sim1* expressions in contrast are not associated with a particular path of cellular differentiation. Rather, both markers molecularly subdivide the dermomyotome and subsequently superimpose this molecular subdivision onto both the myotome and the dermatome.

En1 cells originate from the epaxial dermomyotomal or myotomal precursor pool

En1 expression in the avian somite commences late (somite stages VIII–X) and at a distance to the axial midline tissues, notochord and neural tube, known to control the formation of medial or epaxial somitic derivatives (reviewed by Brent and Tabin, 2002). Thus, it was unclear whether *En1* expression belongs to the epaxial programme of the somite. Consequently, we could not decide whether the *En1–Sim1* expression boundary might demarcate the epaxial–hypaxial interface. To clarify this problem, we determined (a) origin and spread of the *En1*-expressing cells and (b) the regulation of *En1* expression by signals associated with epaxial and hypaxial pathways.

Using DiI–DiO labelling and orthotopic grafting of quail third, half or two third segmental plates into chick hosts, we identified the dorsomedial wall of the somite as source of *En1* precursor cells. Thus, these cells stem from the common epaxial dermomyotomal–myotomal precursor pool, which was proposed by Denetclaw and Ordahl (2000) and Ordahl et al. (2001). During the subsequent stages of dorsomedial–ventrolateral outgrowth of the dermomyotome (Ben-Yair et al., 2003), the *En1* domain expands considerably. Thus, we had to consider that parts of the hypaxial area may have been incorporated into the *En1* domain, casting again doubt on the reliability of *En1* as epaxial marker. Both our labelling and grafting experiments however show that the *En1* zone enlarges due to the growth of the dorsomedial dermomyotomal proper with an additional contribution of cells from the dorsomedial dermomyotomal lip. Importantly, medial-third segmental plate grafts even after prolonged incubation always aligned with the lateral border of *En1* expression. Thus, while we cannot exclude that individual cells may cross from the *Sim1* into the *En1* territory, similar to violators of rhombomere boundaries (Birgbauer and Fraser, 1994), the bulk of *En1* cells is and remains part of the epaxial programme of the somite.

En1 expression is positively regulated by the axial midline tissues and the surface ectoderm

To investigate the regulation of *En1* expression, we systematically manipulated the environment of the paraxial mesoderm at the level of segmental plate (before the specification of the epaxial dermomyotomal–myotomal precursor pool), somites V–VIII (before the onset of *En1* expression) and somites XII–XV (after the initiation of *En1* expression). We found that *En1* failed to be expressed, when notochord and floor plate were ablated at the level of the segmental plate. The removal of the dorsal neural tube prevented *En1* expression, when the operation was performed at segmental plate–somites V–VIII levels before the embryos reached HH14–15. This finding is in line with experiments in the mouse, demonstrating that dorsal neural tube mutants lack somitic *En1* expression (Ikeya and Takada, 1998). Thus, the development of *En1* precursor cells depends on the very same signals that control epaxial myogenesis, reinforcing that *En1* cells are part of the epaxial somitic programmes.

As notochord and neural tube act early, they do not account for the transcriptional activation of the *En1* gene. However, when we separated the somite from the overlying surface ectoderm, *En1* expression was lost at all stages and for operations at segmental plate levels, somites V–VIII and somites XII–XV levels, in line with Olivera–Martinez (2002). Significantly, when the spatiotemporal signalling of tissues required for *En1* expression was altered, such that

the epaxial dermomyotomal–myotomal precursors developed in an ectopic, ventral position (Dietrich et al., 1997, and this study), *En1* was also lacking. This suggests that the ectodermal signals do not act long-range, in line with Fan and Tessier-Lavigne (1994). Rather, the newly specified *En1* precursors have to be brought into contact with the surface ectoderm, which then initiates and maintains expression of *En1*.

The signals involved in positive En1 regulation are Shh and Wnt1/Wnt1-like signals

Our ablation experiments identified notochord, dorsal neural tube and surface ectoderm as key regulators of *En1* cell development. Past studies established Shh as notochord–floor plate-derived signal while Wnt1 mimics most functions of the dorsal neural tube (reviewed by Brent and Tabin, 2002). The signalling from ectoderm to the somite is not fully understood, but based on the panectodermal expression of *Wnt6* in the embryo (Schubert et al., 2002), the ability of Wnt6 and Wnt7a to mimic the ectoderm-driven induction of *Pax3* and *MyoD* in vitro (Fan et al., 1997; Tajbakhsh et al., 1998) and the ability of Wnt6 to mimic ectodermal signalling when expressed from NIH3T3 cells (Schmidt et al., 2004), these Wnt molecules have been proposed as ectodermal signals. Our experiments demonstrate that Shh-loaded beads restore *En1* expression upon ablation of notochord and floor plate. Likewise, cell-expressing Wnt1, but not cells expressing Wnt5a/5b/6/7a, restored *En1* expression following the ablation of the dorsal neural tube. However, when the ectoderm was ablated, again only Wnt1-expressing cells induced or reinstated *En1* expression.

Tissue recombination experiments have shown that ectodermal signalling requires cell–cell contact, while the dorsal neural tube provides diffusible signals (Fan and Tessier-Lavigne, 1994). Moreover, many Wnt proteins tightly associate with the extracellular matrix, limiting the range of their activity (reviewed by Cumberledge and Reichsman, 1997). It is therefore conceivable that the panectodermal factor Wnt6 (Schubert et al., 2002) and Wnt7a, normally expressed in the ectoderm overlying flank and limbs (Yang and Niswander, 1995), have not been presented appropriately by the engineered cell lines to trigger expression of *En1* after ectoderm ablation. Alternatively, cofactors essential for Wnt6 signalling may be absent in RatB1a or DF1 cells used in this study but present in NIH3T3 cells used by Schmidt et al. (2004). Interestingly, bioinformatical sequence comparison suggested that the closest relative to Wnt6 is Wnt1, which signals via the canonical pathway (Schubert et al., 2002; reviewed by Miller, 2002). In our experiments, Wnt1 can replace the function of the ectoderm as *En1* inducer. This suggests that it is a Wnt1-like, βcatenin-mediated signalling event that controls the activation and maintenance of *En1* expression.

En1 expression is suppressed by BMP4

The activation of hypaxial programmes and the simultaneous suppression of epaxial programmes in the lateral somite half depends on BMP4 released by the lateral plate mesoderm (reviewed by Parkyn et al., 2002). We therefore reasoned that if *En1* expression is part of the epaxial programmes, its expression should be negatively regulated by BMP4. Indeed, when the somite was separated from the BMP4-expressing lateral mesoderm, the *En1* domain expanded and reached the lateral edge of the dermomyotome. Implanted BMP4 beads on the other hand readily overcompensated for the absence of the lateral mesoderm and suppressed the expression of *En1*. This suggests that *En1* is under negative control by the lateral mesoderm via BMP4.

The roof plate of the neural tube is a further source of BMP4 signals, which negatively regulates epaxial myogenesis until, induced by BMP4 itself, the BMP inhibitor Noggin is up-regulated in the dml (Sela-Donenfeld and Kalcheim, 2002). We found that *En1* is extremely sensitive to BMP4 as the overcompensation for the lateral mesoderm removal occurred at BMP4 concentrations as low as 10 μg/ml. This finding suggests a scenario for the late onset of *En1* expression at a distance to the axial midline tissues: *En1* may be kept silent in epaxial dermomyotome until this tissue grew sufficiently to allow the most lateral cells to escape the reach of roof-plate-derived BMP4.

En1 and Sim1 molecularly define the epaxial–hypaxial interface

Our study shows that cells to express *En1* originate from the epaxial dermomyotomal–myotomal precursor pool; they are positively regulated by notochord or floor plate (Shh), dorsal neural tube (Wnt1) and surface ectoderm (possibly βcatenin-mediated Wnt signalling) and negatively regulated by BMP4 from the lateral plate mesoderm and possibly, the roof plate (model for the temporospatial regulation of *En1* expression in Fig. 9). *Sim1*-expressing cells originate from the lateral somite half, are positively regulated by the lateral mesoderm (BMP4) and negatively regulated by the dorsal neural tube (Wnt1; Hirsinger et al., 1997; Marcelle et al., 1997; Pourquié et al., 1996). This firmly places *En1* into the epaxial, and *Sim1* into the hypaxial programmes of somite development. We therefore conclude that *En1* and *Sim1* expression molecularly defines the epaxial–hypaxial boundary in the avian somite.

Earlier anatomical studies suggested that the ectodermal thickening called ectodermal notch or furrow may serve as a landmark for the epaxial–hypaxial boundary (Christ et al., 1983). Importantly, this landmark does not coincide with the expression boundary of *En1* and *Sim1*. Rather, it resides at the border between the dermatomal and lateral mesoderm-based expression of *Alx4*, possibly demarcating the border between somitic and nonsomitic dermis. Likewise, the

ectodermal notch marks the point where the myotome entered the lateral mesoderm, possibly discriminating between the primaxial and abaxial component of the hypaxial musculature (Burke and Nowicki, 2003).

En1 and Sim1 cells may set up a functional epaxial–hypaxial compartment boundary

Genetic studies in the mouse and lineage tracing in the chick suggested that epaxial and hypaxial muscle precursors represent distinct somitic cell lineages (Eloy-Trinquet and Nicolas, 2002; Freitas et al., 2001; Selleck and Stern, 1991). In line with this view, our dye labelling and quail-chick grafting experiments indicate that little cell movement occurs between the *En1*- and *Sim1*-expressing domains of the dermomyotome. We therefore asked whether the *En1*–*Sim1* expression boundary may represent a true compartment boundary. Employing cell aggregation assays, it has been demonstrated that cell populations, which form a boundary between them, sort by the means of preferential cell adhesion: the cells adhere to their own kind but avoid cells from across the border (Wizenmann and Lumsden, 1997). We found this also holds true for *En1*- and *Sim1*-expressing cells in the dermomyotome. *En1*-positive epaxial cells mixed freely with epaxial cells, *Sim*-1-positive hypaxial cells mixed with hypaxial cells, but *En1* or epaxial cells sorted from hypaxial cells expressing *Sim1*. This suggests differential adhesion of cells across the epaxial–hypaxial boundary, possibly a prerequisite for the future segregation of muscle and the formation of the lateral myoseptum. Given that *En1* and *Sim1* are transcriptional regulators, we can speculate that they may regulate the epaxial–hypaxial distribution of adhesion molecules.

Do En1 cells play an evolutionarily conserved role in epaxial–hypaxial boundary formation?

Our study suggests that in amniotes, *En1*-expressing cells demarcate the epaxial side of the epaxial–hypaxial boundary. In the zebrafish embryo, *En1*-expressing adaxial cells also set up the epaxial–hypaxial boundary (Halpern et al., 1993; reviewed by Stickney et al., 2000). Both zebrafish and amniotes have in common that the *En1*-expressing cells originate from a precursor cell population close to the axial midline tissues, the medial wall of the somite in the amniote (this study) and the adaxial cells in the fish (Ekker et al., 1992; Felsenfeld et al., 1991; Hatta et al., 1991). Moreover, both cell populations depend on notochord-derived Shh for their development (Currie and Ingham, 1996; Halpern et al., 1993; Wolff et al., 2003; this study). Thus, striking

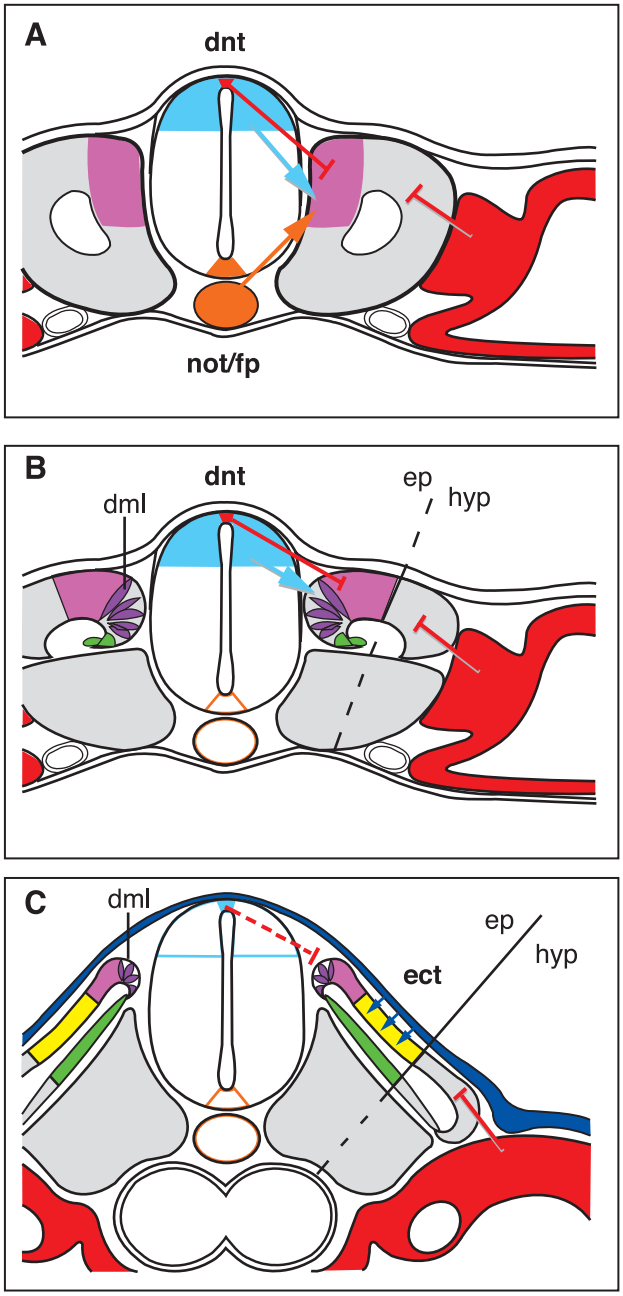

Fig. 9. Model: three-step induction of En1 and the epaxial–hypaxial subdivision of the avian somite. Tissues actively involved in signalling and responding areas of the somites are depicted in colour. Abbreviations: ep, epaxial; hyp, hypaxial; others as in Figs. 1 and 4. (A) Notochord or floor plate (orange; Shh) and dorsal neural tube (turquoise; Wnt1) specify the epaxial myotomal or dermomyotomal precursors (pink) in the dorsomedial wall of the newly formed somite. The lateral mesoderm (red; BMP4) suppresses *En1* in the hypaxial domain of the somite. BMP4 is also provided by the roof plate of the neural tube (red), possibly accounting for the suppression of *En1* in the epaxial precursor cells. (B) In dorsoventrally differentiated somites, the dorsal neural tube (Wnt1) triggers the expansion of the epaxial myotomal or dermomyotomal precursor pool and the differentiation of the first myoblasts (green) from the dml (purple). *En1* remains repressed, possibly due to BMP4 signals from lateral mesoderm and roof plate. (C) The continuous generation of dermomyotomal cells from the dml plus the expansion of the dermomyotome by cell proliferation in situ allows the centrally located epaxial cells to escape the BMP4 signals. Now the ectoderm (dark blue; most likely βcatenin-mediated Wnt signals) can initiate the expression of *En1* (yellow), which in turn, together with *Sim1*, demarcates the epaxial–hypaxial compartment boundary (indicated by solid black line).

similarities exist between amniote and nonamniote *En1* expression at the epaxial–hypaxial border. The main differences are that compared to the fish, amniote *En1* expression commences at late stages of development, and additional signals contribute to the regulation of *En1* expression. Moreover, fish *En1* cells form a thin layer of cells in the middle of the bulky myotome (Felsenfeld et al., 1991, reviewed by Stickney et al., 2000), while the amniote *En1* domain eventually occupies a large territory of dermomyotome, myotome and dermatome. It has to be taken into account, however, that nonamniote vertebrates develop via free-feeding juveniles, which depend on the immediate functionality of their musculoskeletal system (reviewed by Goodrich, 1958). Amniotes by contrast established a direct mode of development, skipping mobile larval stages. This gave room during evolution to delay the differentiation of muscle progenitors, to modify the regulatory cascades for muscle formation and to co-opt additional regulatory cues. Thus, it is well possible that *En1* cells in the amniote somite represent the homologues of the *Engrailed*-expressing adaxial cells in the fish. It cannot be excluded, however, that otherwise unrelated mesodermal cells recruited similar molecular cascades for the formation of the epaxial–hypaxial boundary, rendering the fish and amniote *En1*-expressing cells merely analogous. The identification of the molecular cascades for epaxial–hypaxial boundary formation and the function of *Engrailed* genes in particular is required to in the future clarify this problem.

Acknowledgments

We are indebted to B. Christ for providing insight into the anatomy of the amniote septum laterale and to A. Münsterberg for providing and expression-testing the Wnt-expressing RatB1a cells. We also would like to thank A.-G. Borycki, M. Buckingham, A. Burke, P, Currie, S. Devoto, J. Eisen, A. Graham, S. Hughes, P. Ingham, C. Kalcheim, S. Kuratani, C. Kimmel, A. Münsterberg, C. Ordahl, P. Rigby, R. Spörle and M. Westerfield for stimulating discussions on the evolutionary relationship of the fish and amniote epaxial–hypaxial border. We are most grateful to U. Drescher, M. Ensini, A. Lumsden, F. Schubert, C. Stern, A. Streit, D. Wilkinson and A. Wizenmann for technical advice and F. Schubert for critically reading the manuscript. We thank C.-M. Fan, T. Lints, C. Logan, T. Nohno and T. Ogura for the generous gift of in situ probes.

The work was supported by the Royal Society and the BBSRC.

References

Alvares, L.E., Schubert, F.R., Thorpe, C., Mootoosamy, R.C., Cheng, L., Parkyn, G., Lumsden, A., Dietrich, S., 2003. Intrinsic, Hox-dependent cues determine the fate of skeletal muscle precursors. Dev. Cell 5, 379–390.

Ben-Yair, R., Kahane, N., Kalcheim, C., 2003. Coherent development of dermomyotome and dermis from the entire mediolateral extent of the dorsal somite. Development 130, 4325–4336.

Birgbauer, E., Fraser, S.E., 1994. Violation of cell lineage restriction compartments in the chick hindbrain. Development 120, 1347–1356.

Borycki, A.-G., Mendham, L., Emerson Jr., C.P., 1998. Control of somite patterning by sonic hedgehog and its downstream signal response genes. Development 125, 777–790.

Borycki, A.-G., Brunk, B., Tajbakhsh, S., Buckingham, M., Chiang, C., Emerson Jr., C.P., 1999. Sonic hedgehog controls epaxial muscle determination through Myf5 activation. Development 126, 4053–4063.

Brent, A.E., Tabin, C.J., 2002. Developmental regulation of somite derivatives: muscle, cartilage and tendon. Curr. Opin. Genet. Dev. 12, 548–557.

Burke, A.C., Nowicki, J.L., 2003. A new view of patterning domains in the vertebrate mesoderm. Dev. Cell 4, 159–165.

Cauthen, C.A., Berdougo, E., Sandler, J., Burrus, L.W., 2001. Comparative analysis of the expression patterns of Wnts and Frizzleds during early myogenesis in chick embryos. Mech. Dev. 104, 133–138.

Christ, B., Ordahl, C.P., 1995. Early stages of chick somite development. Anat. Embryol. 191, 381–396.

Christ, B., Jacob, M., Jacob, H.J., 1983. On the origin and development of the ventrolateral abdominal muscles in the avian embryo. An experimental and ultrastructural study. Anat. Embryol. 166, 87–101.

Cinnamon, Y., Kahane, N., Kalcheim, C., 1999. Characterization of the early development of specific hypaxial muscles from the ventrolateral myotome. Development 126, 4305–4315.

Cinnamon, Y., Kahane, N., Bachelet, I., Kalcheim, C., 2001. The sub-lip domain—A distinct pathway for myotome precursors that demonstrate rostral–caudal migration. Development 128, 341–351.

Cumberledge, S., Reichsman, F., 1997. Glycosaminoglycans and WNTs: just a spoonful of sugar helps the signal go down. Trends Genet. 13, 421–423.

Currie, P.D., Ingham, P.W., 1996. Induction of a specific muscle cell type by a hedgehog-like protein in zebrafish. Nature 382, 452–455.

Davis, C.A., Holmyard, D.P., Millen, K.J., Joyner, A.L., 1991. Examining pattern formation in mouse, chicken and frog embryos with an En-specific antiserum. Development 111, 287–298.

Denetclaw, W.F., Ordahl, C.P., 2000. The growth of the dermomyotome and formation of early myotome lineages in thoracolumbar somites of chicken embryos. Development 127, 893–905.

Denetclaw, W.F., Christ, B., Ordahl, C.P., 1997. Location and growth of epaxial myotome precursor cells. Development 124, 1601–1610.

Denetclaw Jr., W.F., Berdougo, E., Venters, S.J., Ordahl, C.P., 2001. Morphogenetic cell movements in the middle region of the dermomyotome dorsomedial lip associated with patterning and growth of the primary epaxial myotome. Development 128, 1745–1755.

Dietrich, S., Schubert, F.R., Lumsden, A., 1997. Control of dorsoventral pattern in the chick paraxial mesoderm. Development 124, 3895–3908.

Dietrich, S., Schubert, F.R., Healy, C., Sharpe, P.T., Lumsden, A., 1998. Specification of the hypaxial musculature. Development 125, 2235–2249.

Ekker, M., Wegner, J., Akimenko, M.A., Westerfield, M., 1992. Coordinate embryonic expression of three zebrafish engrailed genes. Development 116, 1001–1010.

Eloy-Trinquet, S., Nicolas, J.F., 2002. Clonal separation and regionalisation during formation of the medial and lateral myotomes in the mouse embryo. Development 129, 111–122.

Fan, C.M., Tessier-Lavigne, M., 1994. Patterning of mammalian somites by surface ectoderm and notochord: evidence for sclerotome induction by a hedgehog homolog. Cell 79, 1175–1186.

Fan, C.M., Lee, C.S., Tessier-Lavigne, M., 1997. A role for WNT proteins in induction of dermomyotome. Dev. Biol. 191, 160–165.

Felsenfeld, A.L., Curry, M., Kimmel, C.B., 1991. The fub-1 mutation blocks initial myofibril formation in zebrafish muscle pioneer cells. Dev. Biol. 148, 23–30.

Freitas, C., Rodrigues, S., Charrier, J.B., Teillet, M.A., Palmeirim, I., 2001. Evidence for medial/lateral specification and positional information within the presomitic mesoderm. Development 128, 5139–5147.

Gardner, C.A., Barald, K.F., 1992. Expression patterns of engrailed-like proteins in the chick embryo. Dev. Dyn. 193, 370–388.

Goodrich, E.S., 1958. Studies on the Structure and Development of Vertebrates. Dover Publications Inc, New York.

Gossler, A., Hrabe de Angelis, M., 1998. Somitogenesis. Curr. Top. Dev. Biol. 38, 225–287.

Goulding, M., Lamar, E., 2000. Neuronal patterning: making stripes in the spinal cord. Curr. Biol. 10, R565–R568.

Goulding, M., Lumsden, A., Paquette, A.J., 1994. Regulation of Pax-3 expression in the dermomyotome and its role in muscle development. Development 120, 957–971.

Gray, H., 1995. Gray's Anatomy. (thirty-eighth ed.). Churchill Livingstone, Edinburgh, London.

Hadchouel, J., Carvajal, J.J., Daubas, P., Bajard, L., Chang, T., Rocancourt, D., Cox, D., Summerbell, D., Tajbakhsh, S., Rigby, P.W., Buckingham, M., 2003. Analysis of a key regulatory region upstream of the Myf5 gene reveals multiple phases of myogenesis, orchestrated at each site by a combination of elements dispersed throughout the locus. Development 130, 3415–3426.

Halpern, M.E., Ho, R.K., Walker, C., Kimmel, C.B., 1993. Induction of muscle pioneers and floor plate is distinguished by the zebrafish no tail mutation. Cell 75, 99–111.

Hamburger, V., Hamilton, H.L., 1951. A series of normal stages in the development of the chick embryo. J. Morphol. 88, 49–92.

Hatta, K., Bremiller, R., Westerfield, M., Kimmel, C.B., 1991. Diversity of expression of engrailed-like antigens in zebrafish. Development 112, 821–832.

Hirsinger, E., Duprez, D., Jouve, C., Malapert, P., Cooke, J., Pourquié, O., 1997. Noggin acts downstream of Wnt and Sonic Hedgehog to antagonize BMP4 in avian somite patterning. Development 124, 4605–4614.

Huang, R., Christ, B., 2000. Origin of the epaxial and hypaxial myotome in avian embryos. Anat. Embryol. (Berlin) 202, 369–374.

Ikeya, M., Takada, S., 1998. Wnt signalling from the dorsal neural tube is required for the formation of the medial dermomyotome. Development 125, 4969–4976.

Johnson, R.L., Laufer, E., Riddle, R.D., Tabin, C., 1994. Ectopic expression of sonic hedgehog alters dorsal–ventral patterning of somites. Cell 79, 1165–1173.

Kahane, N., Cinnamon, Y., Kalcheim, C., 1998. The origin and fate of pioneer myotomal cells in the avian embryo. Mech. Dev. 74, 59–73.

Kahane, N., Cinnamon, Y., Kalcheim, C., 1998. The cellular mechanism by which the dermomyotome contributes to the second wave of myotome development. Development 125, 4259–4271.

Kahane, N., Cinnamon, Y., Bachelet, I., Kalcheim, C., 2001. The third wave of myotome colonization by mitotically competent progenitors: regulating the balance between differentiation and proliferation during muscle development. Development 128, 2187–2198.

Kahane, N., Cinnamon, Y., Kalcheim, C., 2002. The roles of cell migration and myofiber intercalation in pattern formation of the post-mitotic myotome. Development 129, 2675–2687.

Logan, C., Hanks, M.C., Noble-Topham, S., Nallainathan, D., Provart, N.J., Joyner, A.L., 1992. Cloning and sequence comparison of the mouse, human, and chicken engrailed genes reveal potential functional domains and regulatory regions. Dev. Genet. 13, 345–358.

Marcelle, C., Stark, M.R., Bronner-Fraser, M., 1997. Coordinate actions of BMPs, Wnts, Shh and Noggin mediate patterning of the dorsal somite. Development 124, 3955–3963.

Miller, J.R., 2002. The Wnts. Genome Biol. 3 (REVIEWS3001).

Münsterberg, A., Lassar, A., 1995. Combinatorial signals from the neural tube, floor plate and notochord induce myogenic bHLH gene expression in the somite. Development 121, 651–660.

Münsterberg, A.E., Kitajewski, J., Bumcrot, D.A., McMahon, A.P., Lassar, A.B., 1995. Combinatorial signalling by sonic hedgehog and Wnt family members induces myogenic bHLH gene expression in the somite. Genes Dev. 9, 2911–2922.

Olivera-Martinez, I., Missier, S., Fraboulet, S., Thelu, J., Dhouailly, D., 2002. Differential regulation of the chick dorsal thoracic dermal progenitors from the medial dermomyotome. Development 129, 4763–4772.

Ordahl, C.P., Le Douarin, N.M., 1992. Two myogenic lineages within the developing somite. Development 114, 339–353.

Ordahl, C.P., Berdougo, E., Venters, S.J., Denetclaw Jr., W.F., 2001. The dermomyotome dorsomedial lip drives growth and morphogenesis of both the primary myotome and dermomyotome epithelium. Development 128, 1731–1744.

Palmeirim, I., Henrique, D., Ish-Horowicz, D., Pourquié, O., 1997. Avian hairy gene expression identifies a molecular clock linked to vertebrate segmentation and somitogenesis. Cell 91, 639–664.

Parkyn, G., Mootoosamy, R.C., Cheng, L., Thorpe, C., Dietrich, S., 2002. Hypaxial muscle development. Results Probl. Cell Differ. 38, 127–141.

Pourquié, O., 1999. Notch around the clock. Curr. Opin. Genet. Dev. 9, 559–565.

Pourquié, O., 2003. The segmentation clock: converting embryonic time into spatial pattern. Science 301, 328–330.

Pourquié, O., Fan, C.M., Coltey, M., Hirsinger, E., Watanabe, Y., Bréant, C., Francis-West, P., Brickell, P., Tessier-Lavigne, M., Le Douarin, N.M., 1996. Lateral and axial signals involved in avian somite patterning: a role for BMP4. Cell 84, 461–471.

Ruiz I Altaba, A., Warga, R.M., Stern, C.D., 1993. Fate maps and cell lineage analysis. In: Stern, C.D., Holland, P.W.H. (Eds.), Essential Developmental Biology. Oxford Univ. Press, Oxford, pp. 81–96.

Schmidt, C., Stoeckelhuber, M., McKinnell, I., Putz, R., Christ, B., Patel, K., 2004. Wnt6 regulates the epithelialisation process of the segmental plate mesoderm leading to somite formation. Dev. Biol. 271, 198–209.

Schubert, F.R., Mootoosamy, R.C., Walters, E.H., Graham, A., Tumiotto, L., Münsterberg, A.E., Lumsden, A., Dietrich, S., 2002. Wnt6 marks sites of epithelial transformations in the chick embryo. Mech. Dev. 114, 143–148.

Sela-Donenfeld, D., Kalcheim, C., 2002. Localized BMP4-noggin interactions generate the dynamic patterning of noggin expression in somites. Dev. Biol. 246, 311–328.

Selleck, M.A., Stern, C.D., 1991. Fate mapping and cell lineage analysis of Hensen's node in the chick embryo. Development 112, 615–626.

Šošic, D., Brand-Saberi, B., Schmidt, C., Christ, B., Olson, E.N., 1997. Regulation of paraxis expression and somite formation by ectoderm-and neural tube-derived signals. Dev. Biol. 185, 229–243.

Spörle, R., 2001. Epaxial-adaxial-hypaxial regionalisation of the vertebrate somite: evidence for a somitic organiser and a mirror-image duplication. Dev. Genes Evol. 211, 198–217.

Stickney, H.L., Barresi, M.J., Devoto, S.H., 2000. Somite development in zebrafish. Dev. Dyn. 219, 287–303.

Tajbakhsh, S., Borello, U., Vivarelli, E., Kelly, R., Papkoff, J., Duprez, D., Buckingham, M., Cossu, G., 1998. Differential activation of Myf5 and MyoD by different Wnts in explants of mouse paraxial mesoderm and the later activation of myogenesis in the absence of Myf5. Development 125, 4155–4162.

Takahashi, M., Tamura, K., Buscher, D., Masuya, H., Yonei-Tamura, S., Matsumoto, K., Naitoh-Matsuo, M., Takeuchi, J., Ogura, K., Shiroishi, T., Ogura, T., Belmonte, J.C., 1998. The role of Alx-4 in the establishment of anteroposterior polarity during vertebrate limb development. Development 125, 4417–4425.

Tanda, N., Ohuchi, H., Yoshioka, H., Noji, S., Nohno, T., 1995. A chicken Wnt gene, Wnt-11, is involved in dermal development. Biochem. Biophys. Res. Commun. 211, 123–129.

Wizenmann, A., Lumsden, A., 1997. Segregation of rhombomeres by differential chemoaffinity. Mol. Cell. Neurosci. 9, 448–459.

Wolff, C., Roy, S., Ingham, P.W., 2003. Multiple muscle cell identities induced by distinct levels and timing of hedgehog activity in the zebrafish embryo. Curr. Biol. 13, 1169–1181.

Wurst, W., Auerbach, A.B., Joyner, A.L., 1994. Multiple developmental defects in Engrailed-1 mutant mice: an early mid-hindbrain deletion and patterning defects in forelimbs and sternum. Development 120, 2065–2075.

Yang, Y., Niswander, L., 1995. Interaction between the signaling molecules WNT7a and SHH during vertebrate limb development: dorsal signals regulate anteroposterior patterning. Cell 80, 939–947.